

RESEARCH ARTICLE

Linking Aβ42-Induced Hyperexcitability to Neurodegeneration, Learning and Motor Deficits, and a Shorter Lifespan in an Alzheimer's Model

Yong Ping¹✉, Eu-Teum Hahm²✉, Girma Waro²✉, Qian Song¹✉, Dai-An Vo-Ba², Ashley Licursi², Han Bao¹, Logan Ganoe², Kelly Finch², Susan Tsunoda²*

1 Bio-X Institutes, Key Laboratory for the Genetics of Developmental and Neuropsychiatric Disorders (Ministry of Education), Shanghai Jiao Tong University, Shanghai, China, **2** Department of Biomedical Sciences, Colorado State University, Fort Collins, Colorado, United States of America

✉ These authors contributed equally to this work.

* susan.tsunoda@colostate.edu



OPEN ACCESS

Citation: Ping Y, Hahm E-T, Waro G, Song Q, Vo-Ba D-A, Licursi A, et al. (2015) Linking Aβ42-Induced Hyperexcitability to Neurodegeneration, Learning and Motor Deficits, and a Shorter Lifespan in an Alzheimer's Model. *PLoS Genet* 11(3): e1005025. doi:10.1371/journal.pgen.1005025

Editor: Pedro Fernandez-Funez, University of Florida, UNITED STATES

Received: October 13, 2014

Accepted: January 25, 2015

Published: March 16, 2015

Copyright: © 2015 Ping et al. This is an open access article distributed under the terms of the [Creative Commons Attribution License](https://creativecommons.org/licenses/by/4.0/), which permits unrestricted use, distribution, and reproduction in any medium, provided the original author and source are credited.

Data Availability Statement: All relevant data are within the paper and its Supporting Information files.

Funding: This work was funded by the National Institutes of Health: R01 GM083335 (ST) and R03 AG047132 (ST), National Natural Science Foundation of China grant, 81371482 (YP), Science and Technology Commission of Shanghai Municipality grant, 13ZR1456500 (YP) and Innovation Program of Shanghai Municipal Education Commission grant, 14ZZ028 (YP). The funders had no role in study design, data collection and analysis, decision to publish, or preparation of the manuscript.

Abstract

Alzheimer's disease (AD) is the most prevalent form of dementia in the elderly. β-amyloid (Aβ) accumulation in the brain is thought to be a primary event leading to eventual cognitive and motor dysfunction in AD. Aβ has been shown to promote neuronal hyperactivity, which is consistent with enhanced seizure activity in mouse models and AD patients. Little, however, is known about whether, and how, increased excitability contributes to downstream pathologies of AD. Here, we show that overexpression of human Aβ42 in a *Drosophila* model indeed induces increased neuronal activity. We found that the underlying mechanism involves the selective degradation of the A-type K⁺ channel, Kv4. An age-dependent loss of Kv4 leads to an increased probability of AP firing. Interestingly, we find that loss of Kv4 alone results in learning and locomotion defects, as well as a shortened lifespan. To test whether the Aβ42-induced increase in neuronal excitability contributes to, or exacerbates, downstream pathologies, we transgenically over-expressed Kv4 to near wild-type levels in Aβ42-expressing animals. We show that restoration of Kv4 attenuated age-dependent learning and locomotor deficits, slowed the onset of neurodegeneration, and partially rescued premature death seen in Aβ42-expressing animals. We conclude that Aβ42-induced hyperactivity plays a critical role in the age-dependent cognitive and motor decline of this Aβ42-*Drosophila* model, and possibly in AD.

Author Summary

Alzheimer's disease (AD) is the most prevalent form of dementia in the elderly population. While it is established that β-amyloid (Aβ) peptide accumulation is a primary event leading to AD, there is little known about how Aβ induces progressive neurodegeneration and decline in cognitive and motor function. Recently, over-production of Aβ has been shown to

Competing Interests: The authors have declared that no competing interests exist.

result in increased neuronal excitability, and Ca²⁺ “overload”, in hippocampal and cortical neurons. Increased excitability is also consistent with behavioral studies which have shown enhanced seizure activity in mouse models with increased A β expression, and increased risk of epilepsy in AD patients. We use a transgenic *Drosophila* model that expresses the secreted human A β 42; this A β 42-*Drosophila* line exhibits many of the hallmarks of AD. We show that the A β 42-*Drosophila* line also displays increased neuronal excitability. We determine that the increase in excitability is due to the degradation of a specific K⁺ channel, K_v4. We then show that genetic restoration of K_v4 attenuates age-dependent learning and locomotor deficits, slows the onset of neurodegeneration, and partially rescues premature death seen in A β 42-expressing animals. We conclude that A β 42-induced hyperactivity plays a critical role in the age-dependent cognitive and motor decline of this A β 42-*Drosophila* model, and possibly in AD.

Introduction

The accumulation of β -amyloid (A β) oligomers in the brain has strongly been implicated as a primary event in the progression of Alzheimer's disease (AD) [1–4]. While many studies have shown that A β induces excitatory synaptic depression [5,6], more recent reports suggest that A β expression also leads to neuronal hyperactivity in cortical and hippocampal neurons [7–13]. Interestingly, increased excitability and Ca²⁺ overload are correlated with neurons in the vicinity of A β plaques [9,10]. Much remains to be understood about how A β induces both hypo- and hyperactivity, and how these changes are temporally coordinated in the pathogenesis of AD. Some reports suggest that soluble and protofibrillar A β induce early hyperactivity that precedes neuronal silencing [7,8,12].

While increased excitability is consistent with enhanced seizure activity in A β expressing mouse models [7,11] and increased risk of epilepsy in AD patients [14], it is unknown whether, and to what extent, hyperactivity contributes to downstream effects associated with A β accumulation, such as impaired cognitive and motor function. In this study, our intent was to restore excitability to an A β -expressing model system and examine whether these age-associated effects would be ameliorated *in vivo*. To do this, it was critical to first identify key mechanism(s) by which excitability is increased by A β . A few reports have identified potential contributors to A β -induced hyperactivity. For example, neocortical pyramidal cells and dentate granule cells from mice overexpressing A β have been observed to have a more depolarized resting potential, resulting in lower action potential thresholds and increased bursts of firing [11]. An increase in spike afterdepolarization has been reported in CA1 pyramidal neurons from transgenic mice overexpressing A β [13]. More recently, a transgenic mouse line expressing high levels of human A β has been reported to have decreased levels of the voltage-gated Na⁺ channel, Na_v1.1, in parvalbumin inhibitory interneurons [15].

Here, we use a transgenic *Drosophila* line that over-expresses a secreted form of the toxic human A β _{1–42} (A β 42). These flies exhibit many of the pathogenic hallmarks associated with AD: extracellular amyloid deposits, age-dependent learning and locomotor defects, progressive neurodegeneration and premature death [16–18]. We first show that expression of human A β 42 indeed induces neuronal hyperexcitability. Since fly brains do not share the same circuitry or complexity of mammalian systems, examining underlying circuit changes would not be meaningful. Intrinsic changes, however, are more likely to be conserved and easier to genetically “reverse”. In addition, while virtually all ion channel families are represented in flies, many families are distilled to a single gene in flies, making intrinsic changes more easily detectable. We

characterized A β 42-induced changes in excitability and show that these changes are explained by selective degradation of the highly conserved A-type K⁺ channel, K_v4. We then transgenically increased K_v4 to wild-type levels in A β 42-expressing animals. We show that when excitability is restored, nearly all A β 42-induced downstream effects including, neurodegeneration, locomotor and learning defects, and premature death, were attenuated, and in some cases, fully rescued.

Results

Characterizing A β 42-Induced Hyperexcitability

In this study, we used a transgenic line expressing human A β 42 fused to an N-terminal rat preproenkephalin signal peptide that has been shown by two different groups to direct expression, cleavage of the signal sequence, and extracellular secretion of A β 42 [16,17], thereby mimicking human A β 42 accumulation in the extracellular space around neurons. This sequence was placed under the control of an *upstream activating sequence* (UAS), UAS-A β 42 [18]. Using the UAS-GAL4 system in *Drosophila* [19], UAS-A β 42 expression was activated with the pan neuronal driver *elav-GAL4* (*elav-GAL4;UAS-A β 42/+*). We first examined if these neurons from A β 42-secreting cultures displayed increased excitability. We performed current-clamp recordings from primary neurons that were dissociated from late-gastrula stage embryos and grown for up to two weeks in culture. These neurons likely represent larval stage neurons and are among the best characterized neurons in *Drosophila* with respect to voltage-dependent channels and synaptic physiology [20–26].

We grew cultures in 20 μ L drops of media and aged them for 9 days to allow for A β 42 expression, secretion, and accumulation; A β 42 expression/accumulation was confirmed by immunoblot analyses (Fig. 1A) and immunostaining of cultures (Fig. 1B). No differences in neuronal growth could be seen between A β 42-expressing cultures and control cultures (Fig. 1B). We examined action potential (AP) firing in these neurons response to an injection of current ramped from 0 to 150 pA over a 1-second period; pre-injection of current was applied to normalize membrane potentials to -50 to -60 mV (similar to the average resting potential of these cells) before ramped stimulation was applied. We found that neurons from A β 42-expressing/secreting cultures (also referred to as A β 42 neurons) consistently fired more readily, with less current injection, compared to neurons from a genetic background control line (Fig. 1A). AP firing in A β 42 neurons was initiated when ramp stimulation reached only 19.5 \pm 2.2 pA ($n = 6$; Fig. 1B); in contrast, control neurons fired when current injection reached 35.9 \pm 4.7 pA ($n = 13$; Fig. 1B). The charge transfer required for AP firing in A β 42 neurons was less than half of what was needed for wild-type neurons (Fig. 1B). These results suggest that neurons from A β 42-expressing cultures indeed exhibit increased susceptibility to firing.

To further characterize the hyperactivity of A β 42 neurons, we compared AP firing in response to 500 ms current injections in neurons from background control lines and neurons from A β 42-expressing cultures. Current pulses of 40 pA were used to examine the latency to the first AP firing; for neurons that did not fire APs, we increased current injections by 20 pA until APs were elicited. Wild-type neurons displayed a clear negative correlation between membrane potential and latency to the first AP firing (Fig. 1C-D). Interestingly, this latency to the first AP is dependent almost exclusively on K_v4 channels [26], which carry an A-type K⁺ current that is activated at subthreshold potentials. The number of K_v4 channels available for activation is dependent on membrane potential, such that the more depolarized the membrane potential, the smaller the number of K_v4 channels available for activation [21] and therefore, the shorter the latency to AP firing. Neurons from A β 42-expressing cultures, in contrast to wild-type, displayed significantly reduced correlation between membrane potential and latency to AP firing (Fig. 1D). These results suggested that K_v4 channels, in particular, may be impacted by A β 42 expression.

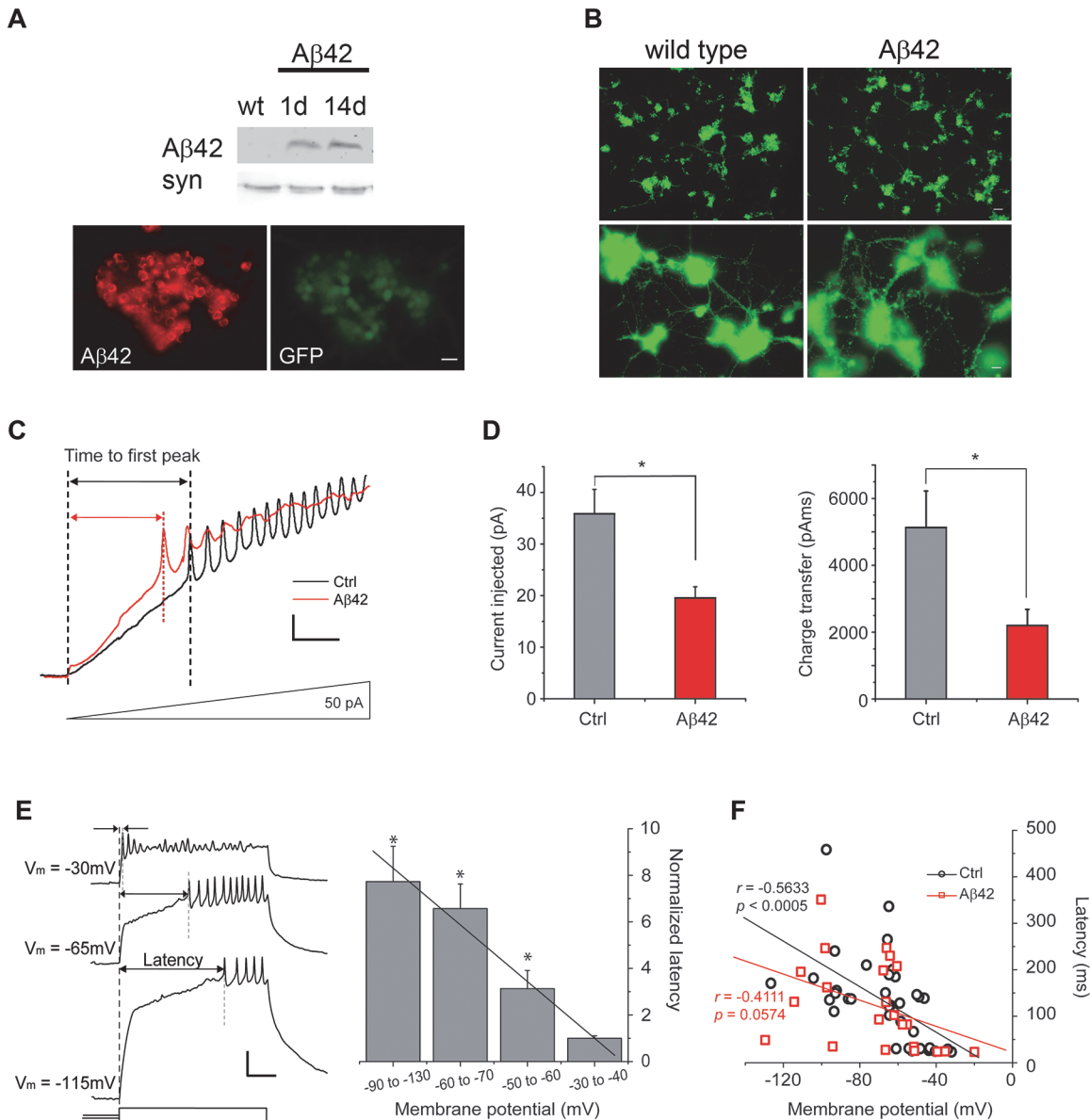


Fig 1. A β 42 induces increased neuronal excitability in cultures 9 days old. (A) Representative immunoblots of fly heads (*Top*) and immunostaining of cultured neurons (*Bottom*) showing expression of A β 42 in *elav-GAL4;UAS-A β 42/+* (A β 42) heads and *elav-GAL4;UAS-A β 42/+;UAS-GFP* neurons, respectively; absence of A β 42 expression in wild-type (wt) is shown as a negative control. Note that immunostaining is from a large cluster of neurons identified by GFP expression. Scale bar represents 12.5 μ m. (B) Shown are representative wild-type and *elav-GAL4;UAS-A β 42/+* (A β 42) cell cultures, both with neurons expressing GFP as a marker, at 9 days. At lower power (*Top*), whole cultures from a single-embryo can be seen (scale bar represents 25 μ m); at higher power (*Bottom*), neuronal processes between clusters of neurons can be seen (scale bar represents 8 μ m). No obvious differences in growth of cultured neurons between wt and A β 42 were observed. (C) Representative current-clamp recordings from wild-type (Ctrl) and *elav-GAL4;UAS-A β 42/+* (A β 42) neurons, showing relative times to the first action potential (AP) firing in response to ramped current stimulation. Current injection was ramped from 0 to 150 pA over 1 sec; voltage responses to the first 336 ms (50 pA) of the ramp protocol are shown. Scale bars represent 50 ms and 10 mV. (D) Quantification of the injected current (*Left*) and the charge transfer (*Right*) required to elicit the first AP in Ctrl and A β 42 neurons during ramp stimulation; all ramp protocols were initiated from a membrane potential of -50 to -60 mV. The average charge transfer to elicit AP firing was also significantly reduced in A β 42 neurons (2197.4 \pm 484.46 pAms, n = 6), compared to Ctrl (5132.8 \pm 1091.32 pAms, n = 13; $P < 0.05$, Student's t-test). (E) Representative traces (*Left*) from a wild-type neuron, showing the latency to AP firing in response to a 500 ms pulse of 20 pA current injection, following pre-injections of current that generated a membrane potential of -115, -65, or -30 mV. Latencies to AP firing was normalized to average latency at -30 to -40 mV are shown for wild-type neurons from the indicated membrane potentials (*Right*). Note the negative correlation between AP latency and membrane potential (* denotes a significant difference in latency compared to that at $V_m = -30$ to -40 mV; $P < 0.05$, Student's t-test). Scale bar represents 100 ms and 20 mV. (F) AP latencies, in response to 500 ms, 40 pA current pulses, from single events are plotted against membrane potential for Ctrl and A β 42 neurons. Ctrl cells showed a significant correlation between latency and membrane potential ($r = -0.5633$, $P < 0.0005$, n = 37), while A β 42 cells did not ($r = -0.4111$, $P = 0.0574$, n = 22); the coefficient of correlation for each genotype was calculated by the Pearson product-moment correlation coefficients (see [Materials and Methods](#)).

doi:10.1371/journal.pgen.1005025.g001

K_v4 Current Is Selectively Decreased by A β 42 Expression

To test the hypothesis that K_v4 channels are affected by A β 42 expression, we performed voltage-clamp studies to examine whether K_v4, or any other voltage-dependent K⁺ currents, were altered in A β 42-expressing cultures. Fortunately, previous studies have genetically identified all of the voltage-dependent K⁺ currents present in these neurons: all of the A-type K⁺ currents (I_A) present in the cell bodies of these neurons are carried by channels encoded by the single K_v4 (*Shal*) gene in *Drosophila*, while the delayed rectifier (DR) component has been shown to be encoded largely by the single K_v2 (*Shab*) gene, and in small part by the K_v3 (*Shaw*) gene [20,21]. The K_v2-K_v3 DR component was recorded using a prepulse of -45 mV to completely inactivate K_v4 channels, before stepping to a depolarized test potential; the K_v4 current was then isolated by subtracting the DR component from the whole-cell current, as performed in previous studies [20,21,25,26]. Since A β 42 is thought to have especially detrimental effects for neurons involved in cognitive function, we focused on Kenyon cells of the mushroom bodies (MBs), which have been shown to constitute the major site of olfactory learning and memory formation in the fly brain [27–30]. To identify MB neurons, we crossed transgenic *elav-GAL4; UAS-A β 42/+* flies to flies containing a *GFP.S65T.T10* transgene, which has been shown to drive GFP expression only in MB neurons, regardless of the *GAL4* driver present [30,31].

We recorded from GFP-labeled MB neurons from 20 μ L drop cultures at 1, 5, and 9 days. We found that the K_v2-K_v3 DR component was increased in A β 42 neurons at 1 day, compared to control neurons from relevant genetic background lines (*UAS-A β 42/+* or *elav-GAL4*); this increase, however, was not persistent after the first day (Figs. 2 and S1). More prominent was a 37% decrease in the K_v4 current density that developed in A β 42 neurons after 9 days compared to controls (Figs. 2 and S1); no differences were seen in cell capacitance (Ctrl: 2.7 \pm 0.2 pF, A β 42: 2.5 \pm 0.1 pF), resting membrane potential (Ctrl: -55.0 \pm 2.3 mV, A β 42: -52.1 \pm 2.6 mV), or input resistance (Ctrl: 2.1 \pm 0.2 G Ω , A β 42: 2.2 \pm 0.2 G Ω). The loss of K_v4 current is consistent with current-clamp recordings that show a loss of correlation between membrane potential and latency to AP firing (Fig. 1D).

We also examined whether the apparent loss of K_v4 current in A β 42-expressing neurons might be due to an A β 42-induced change in K_v4 inactivation or activation properties. We compared steady-state inactivation properties of K_v4 currents in A β 42-expressing neurons and background controls. Whole-cell currents inactivated with more depolarized pre-pulses. As previously characterized, this inactivation was best fit with a double Boltzman equation with the component that inactivates at more hyperpolarized potentials corresponding to the K_v4 current [20,21]. No differences were observed between A β 42-expressing and background controls (Fig. 2C). Activation properties were also not altered by A β 42 expression (Fig. 2D). These results suggest that the A β 42-induced decrease in K_v4 current density is not due to a change in steady-state inactivation or activation properties of the channel.

To examine if A β 42 accumulations seen in these cultures might co-localize with K_v4 channels, we made cultures from *elav-GAL4; UAS-A β 42/UAS-GFP-K_v4* animals and performed co-immunostaining using antibodies against A β 42 and GFP. Interestingly, after 9 days in culture, A β 42 seemed to accumulate especially near the membranes of neurons. Fig. 3A shows anti-A β 42 staining overlapping with GFP-K_v4 labeling, suggesting a direct interaction.

We next examined whether a reduction in the K_v4 current would also be observed in the intact adult brain. Background control lines and transgenic *elav-GAL4; UAS-A β 42/+* flies were aged for 3 or 8 days after eclosion (AE); whole brains were acutely dissected; MB neurons were GFP labeled as described above. No difference in K⁺ current density was observed at 3 days. At 8 days, however, we found that K_v4 current density was significantly reduced in MB neurons from A β 42-expressing brains (Fig. 3B). No differences in cell capacitance (Ctrl: 1.9 \pm 0.1 pF,

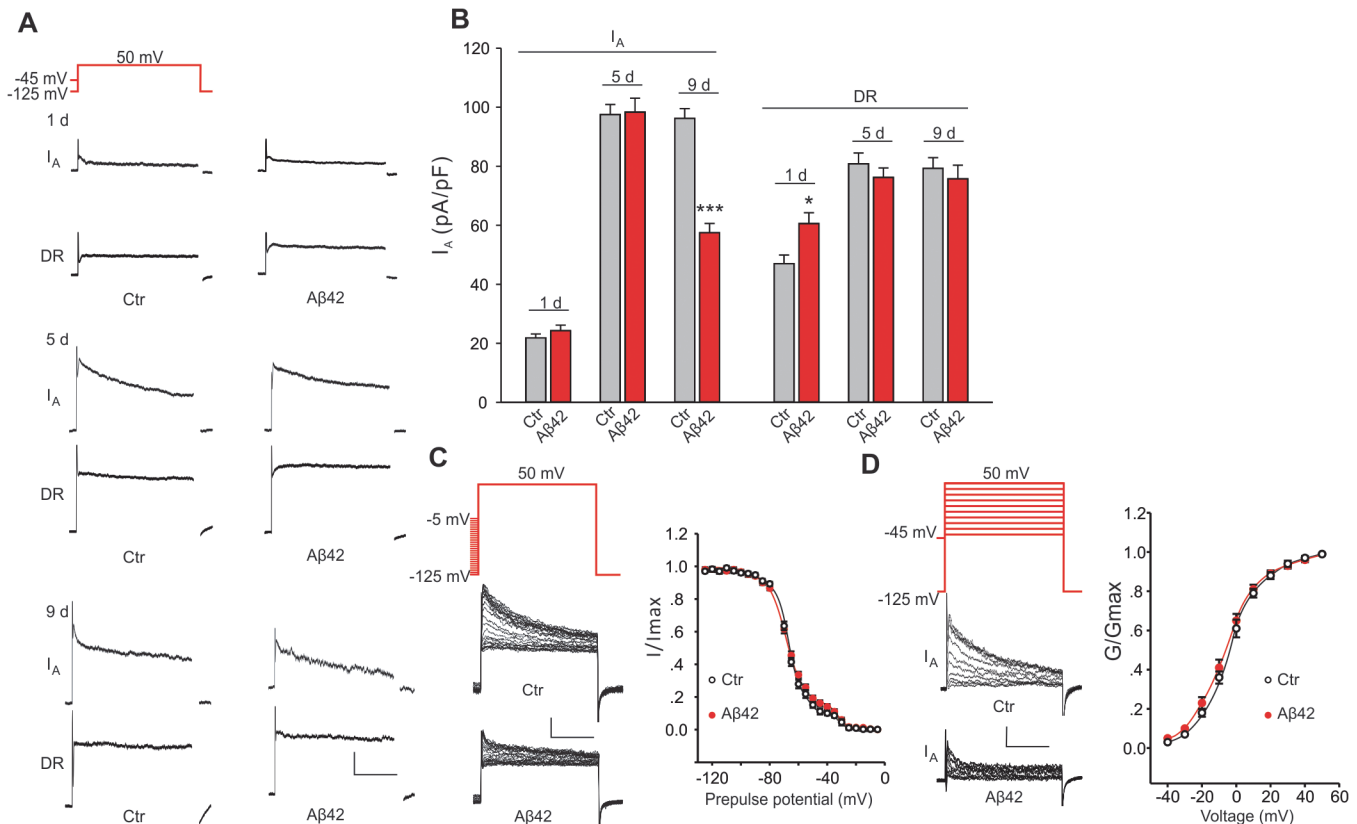


Fig 2. Aβ42-induced changes in voltage-dependent K⁺ currents in primary neurons. Representative K⁺ current traces (A) and quantification of current amplitudes (B) from MB neuron recordings from *UAS-Aβ42/+* (Ctr) and *elav-GAL4;UAS-Aβ42/+* (Aβ42) embryos cultured for 1, 5 and 9 days. The K_v2-K_v3 DR component was recorded using a prepulse of -45 mV to completely inactivate K_v4 channels, before stepping to a test potential of +50 mV; the K_v4 current was then isolated by subtracting this DR component from the total whole-cell current elicited from a prepulse of -125 mV, stepping to a test potential of +50 mV. Current density was obtained by dividing peak current amplitude by cell capacitance. K_v4 current density was significantly reduced in Aβ42 MB neurons in 9-day old cultures, while no difference in K_v2-K_v3 currents was observed. (n = 8–10 for each group, * P < 0.05, ** P < 0.01, Student's t-test). Scale bars, 100 pA, 50 ms. (C-D) Steady-state inactivation and activation properties of Kv4 compared between neurons from Ctr and Aβ42 cultures. For steady-state inactivation analyses, we used a prepulse from -125 to -5 mV, in 5 mV intervals, then stepped to a test potential of +50 mV; representative current traces are shown (C, Left). For G-V analyses, we used voltage jumps from -40 to 50 mV, in 10 mV intervals, and either a prepulse of -125 mV or -45 mV for the total current or DR component, respectively; K_v4 current amplitudes were obtained by subtracting the DR component from the total current. Steady-state inactivation and activation curves were fitted with Boltzmann functions, $I/I_{max} = 1/(1 + \exp[(V - V_{1/2})/k])$ and $G/G_{max} = 1/(1 + \exp[(V_{1/2} - V)/k])$, respectively. V_{1/2} is the half-maximal voltage, and k is the slope factor. Note that steady-state inactivation was fitted by two Boltzmann equations, and K_v4 is represented by the first Boltzmann (more negative operating range) [20,21]. There was no significant difference in half-maximal inactivation potential values (Ctr, V_{1/2} = -69.3 ± 2.1 mV, k = 9.1 ± 0.5; Aβ42, V_{1/2} = -71.2 ± 3.4 mV, k = 9.7 ± 0.5). There was also no difference in the half-maximal activation potential values (Ctr, V_{1/2} = -5.7 ± 0.4 mV, k = 12.5 ± 0.8; Aβ42, V_{1/2} = -6.8 ± 0.4 mV, k = 13.6 ± 0.6). n = 10 or each group. *** P < 0.001. All neurons were from cultures 9 days old.

doi:10.1371/journal.pgen.1005025.g002

Aβ42: 1.8 ± 0.1 pF), resting membrane potential (Ctrl: -52.8 ± 2.3 mV, Aβ42: -49.1 ± 1.7 mV), or input resistance (Ctrl: 2.5 ± 0.1 GΩ, Aβ42: 2.4 ± 0.2 GΩ) were observed between control and Aβ42 neurons. Our results in primary cultures and the intact brain both indicate that the K_v4 current, and not the K_v2-K_v3 DR current, is affected by Aβ42 with age.

Aβ42 Induces Degradation of K_v4 Protein via a Pathway Dependent on Both the Proteasome and Lysosome

To determine if the reduction in K_v4 current is due to a decrease in channel protein, we performed immunoblot analyses on heads from an *elav-GAL4;UAS-Aβ42/+* flies compared to background control lines. Steady-state levels of K_v4 protein were not significantly different at 2–3 days AE. At 7–8 days, however, heads from *elav-GAL4;UAS-Aβ42/+* flies displayed a

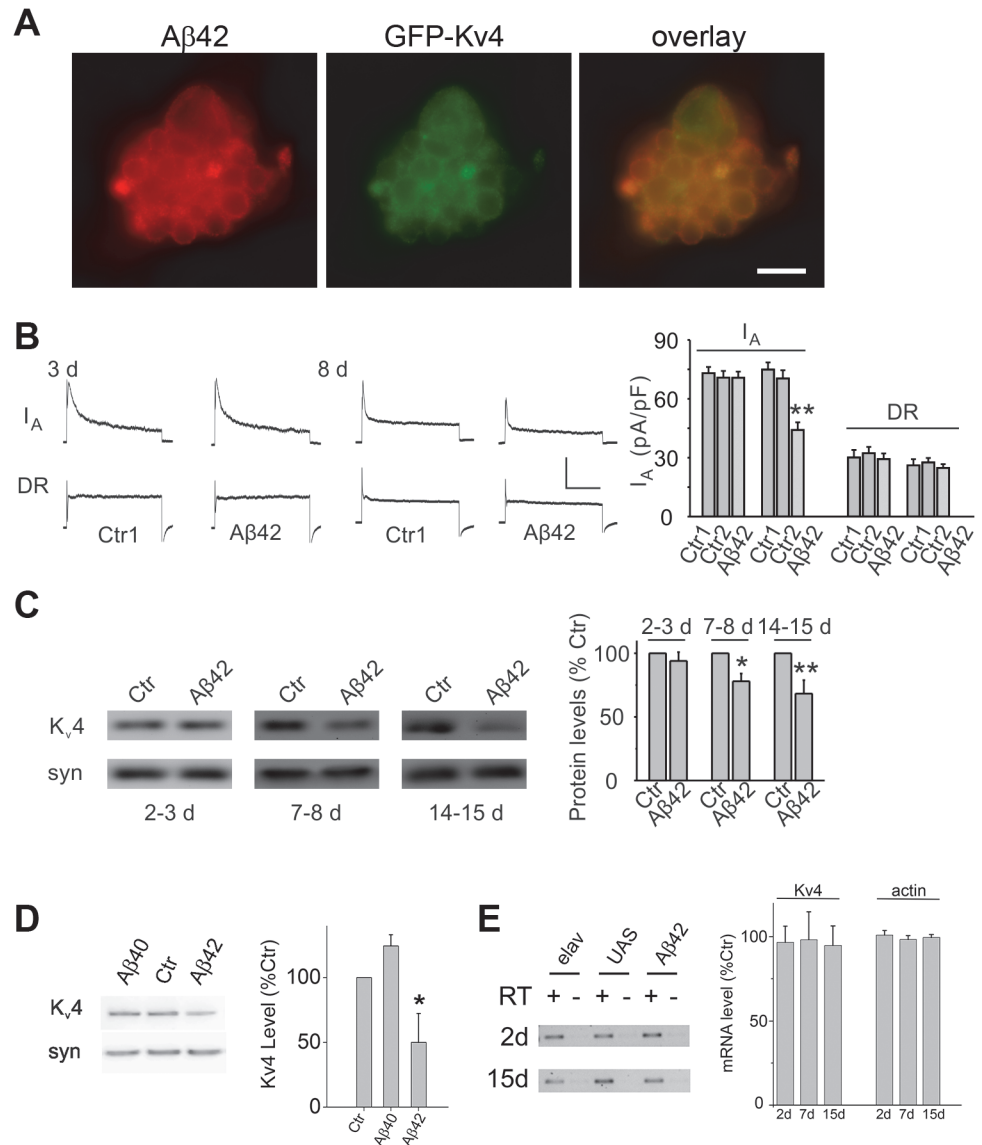


Fig 3. Expression of A β 42 decreases Kv4 protein and currents in the intact brain. (A) Representative neuronal cluster from 9 day old culture from *elav-GAL4;UAS-A β 42/UAS-GFP-Kv4* embryos show co-localization of A β 42 (red) and GFP-Kv4 (green) immunostaining. Scale bar represents 8.3 μ m. (B) Representative Kv4 and Kv2-Kv3 traces (Left), and Kv4 current density quantification (Right) from GFP-labeled MB neurons in *UAS-A β 42/+* (Ctr) and *elav-GAL4;UAS-A β 42/+* (A β 42) intact brains at 3 and 8 days; Ctr1 and Ctr2 on right correspond to *UAS-A β 42/+* and *elav-GAL4/+*, respectively. The Kv2-Kv3 DR component was recorded using a prepulse of -45 mV to completely inactivate Kv4 channels, before stepping to a test potential of +50 mV; the Kv4 current was then isolated by subtracting this DR component from the total whole-cell current elicited from a prepulse of -125 mV, stepping to a test potential of +50 mV. Current density was obtained by dividing peak current amplitude by cell capacitance. Kv4 current density in A β 42 neurons at 8 days were significantly reduced compared to Ctr1 and Ctr2 neurons ($P < 0.05$, $n = 6-13$ for each genotype). Scale bars represent 50 pA and 50 ms. (C) Representative immunoblots (Left) and quantitative analyses (Right) of Kv4 protein levels in *UAS-A β 42/+* (Ctr) and *elav-GAL4;UAS-A β 42/+* (A β 42) heads at 2–3, 7–8, and 14–15 days after eclosion. Protein levels were normalized to the loading control signal from anti-syntaxin (syn) ($n = 4$ for each group, * $P < 0.05$, ** $P < 0.01$, Student's t-test). (D) Representative immunoblots (Left) and quantitative analyses (Right) of Kv4 protein from *elav* (Ctr), *elav;UAS-A β 40/+* (A β 40), and *elav;UAS-A β 42/+* heads at 14–15 days AE. ($n = 3-4$ for each group, * $P < 0.05$, Student's t-test indicates significant difference between A β 40 and A β 42) (E) Representative blots (Left) and quantitative results (Right) from RT-PCR analyses for Kv4 and *actin* RNA levels from *elav* (Ctr), *UAS-A β 42* (UAS), and *elav;UAS-A β 42/+* (A β 42) flies aged 2, 7, and 15 days AE. Quantitation was performed from RT-PCR results from three independent RNA extractions; RT minus controls were always performed in parallel with RT plus reactions as indicated. No significant differences were seen across the three genotypes.

doi:10.1371/journal.pgen.1005025.g003

decrease in K_v4 protein, compared to controls; this decrease continued to persist for at least 14–15 days AE (Figs. 3C and S2). To test whether the decrease in K_v4 was specific to the expression of A β 42, we also examined a similar transgenic line generated to over-express a secreted human A β 40 peptide [16]. We found that steady-state K_v4 protein levels in *elav-GAL4; UAS-A β 40/+* fly heads were not significantly different from background control lines at 14–15 days AE, in contrast to *elav-GAL4; UAS-A β 42/+* heads (Fig. 3D). These results suggest that A β 42, but not A β 40, induces an age-dependent loss of K_v4.

To investigate the mechanism by which K_v4 protein loss occurs in *elav-GAL4; UAS-A β 42/+* flies, we first examined whether mRNA levels of K_v4 were altered by A β 42 expression. We isolated RNA from *elav-GAL4; UAS-A β 42/+* and background controls, *elav/+* and *UAS-A β 42/+*, then performed RT-PCR using primers for K_v4. These experiments were performed using flies that were aged 2 days, 7 days, and 15 days AE; RNA extractions from three different pools of aged flies were used. We found no significant difference in K_v4 mRNA levels from 2 to 15 days (Fig. 3E), suggesting that the reduction in K_v4 is not likely to be due to a change in transcript level.

We next tested the hypothesis that A β 42 induces an increase in K_v4 protein degradation. Since major degradation pathways include the proteasome and/or lysosome, we examined whether A β 42-induced loss of K_v4 required function of either. To test the possible involvement of the proteasome, neurons dissociated from *elav-GAL4; UAS-A β 42/+* and *UAS-A β 42/+* lines were cultured for 9 days in the presence or absence of MG132, which is known to block proteasome function. We found that MG132 completely blocked the A β 42-induced decrease in I_A (Fig. 4A), suggesting that A β 42 induces degradation of K_v4 channels via a proteasome-dependent pathway. To test the proteasome's involvement *in situ*, we dissected brains at 2 days AE, then maintained them in culture for an additional 4–5 days, as previously performed [25]. Dissected *elav-GAL4; UAS-A β 42/+* and *UAS-A β 42/+* brains were mock and MG132-treated for 4 days. Immunoblot analyses showed that A β 42 still induced a 22% decrease in K_v4 protein in cultured brains (Fig. 4B). The decrease, however, was completely blocked in the presence of MG132 (Fig. 4B). We also tested the involvement of the proteasome *in vivo*, using transgenic lines that over-express *Pros26¹* and *Pros β ²*, dominant-negative mutant forms of the 20S proteasome subunits β 6 and β 2, respectively [32]. Flies expressing *Pros26¹* and/or *Pros β ²* alleles have been shown to exhibit normal proteasome function at 18°C, but severely impaired function when shifted to 29°C [33,34]. We raised *elav-GAL4; UAS-Pros26¹/UAS-A β 42; UAS-Pros β ²/+* and *elav-GAL4; UAS-Pros26¹/+; UAS-Pros β ²/+* flies at 18°C during development, then shifted newly-eclosed adult flies to 29°C for 7–8 days. We found that when proteasome activity was inhibited, A β 42 did not induce a decrease in K_v4 protein, as assayed by immunoblot analyses, or a decrease in the K_v4 current, as recorded from MB neurons in the intact brain (Fig. 4C–D). To ensure that an A β 42-induced decrease in K_v4 could still be expected with the temperature-shift protocol used, we performed similar experiments with *elav-GAL4; UAS-A β 42/+* and *UAS-A β 42/+*. A β 42 expression still induced a decrease of K_v4 protein after a temperature shift to 29°C (Fig. 4C). Together, these results strongly suggest that A β 42 induces a loss of K_v4 protein by way of a proteasome-dependent pathway.

Since turnover of other ion channels and receptors have been shown to be dependent on both the proteasome and lysosome [35–38], we also tested for the possible involvement of the lysosome. We used leupeptin, which is known to block lysosomal function, in wild-type and A β 42-expressing neuronal cultures. One day after cell cultures were established, leupeptin was added, and cultures were maintained for another 8 days before recording K_v4 currents. We found that leupeptin, at 20 μ M, blocked the decrease in K_v4 current in A β 42-expressing neurons (Fig. 4E). With 10 μ M leupeptin, however, K_v4 currents were still decreased in A β 42-neurons (Fig. 4E), indicating a concentration dependent block of the decrease in K_v4 current seen

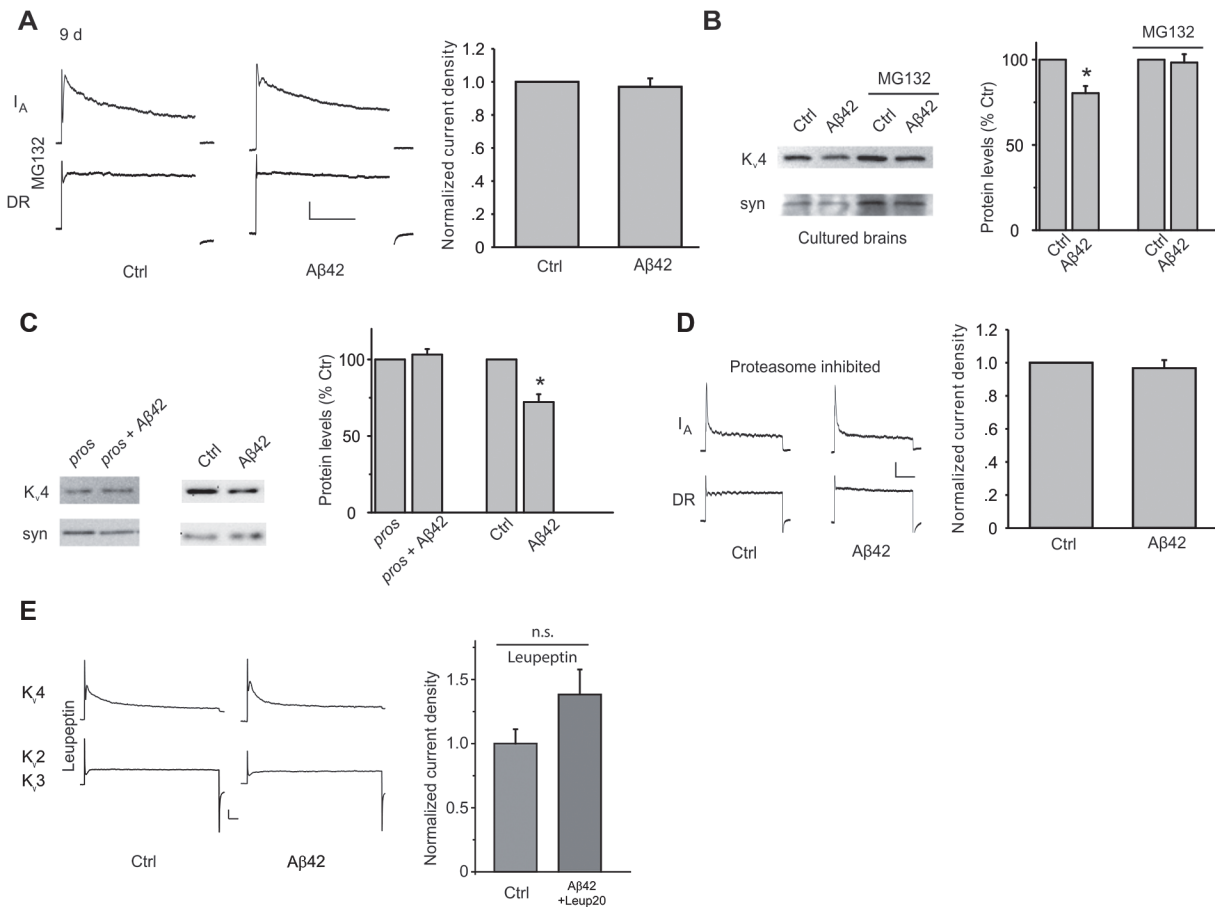


Fig 4. A β 42-induced down-regulation of K_v4 protein is mediated by a proteasome and lysosome-dependent pathway. (A) Representative traces of separated K_v4 and K_v2-K_v3 currents recorded from MB neurons from *UAS-A β 42/+* (Ctrl) and *elav-GAL4;UAS-A β 42/+* (A β 42) cultures at 9 days, after incubation with MG132 (10 μ M). The K_v2-K_v3 DR component was recorded using a prepulse of -45 mV to completely inactivate K_v4 channels, before stepping to a test potential of +50 mV; the K_v4 current was then isolated by subtracting this DR component from the total whole-cell current elicited from a prepulse of -125 mV, stepping to a test potential of +50 mV. Current density was obtained by dividing peak current amplitude by cell capacitance. Quantitative analyses of K_v4 current density shows that MG132 blocked the A β 42-induced down-regulation of K_v4 (Right; n = 8–9 for each group, ** P < 0.01, Student's t-test). Scale bars represent 100 pA and 50 ms. (B) Representative immunoblots and quantitative analyses of K_v4 protein levels in cultured brains. The A β 42-induced decrease in K_v4 is blocked when brains were incubated with MG132 for 4 days. K_v4 levels were normalized to the loading control signal from anti-syntaxin (syn) (n = 3 for each group, * P < 0.05, Student's t-test). (C) Down-regulation of K_v4 protein by A β 42 is absent when proteasome activity was inhibited by expression of the dominant temperature-sensitive *UAS-Pros26¹* and *UASPros β ²* transgenes. *elav-GAL4;UAS-pros26¹/+;UAS-pros β ²/+* flies (pros), *elav-GAL4;UAS-A β 42/UAS-pros26¹;UAS-pros β ²/+* flies (pros + A β 42), *UAS-A β 42/+* (Ctrl), and *elav-GAL4;UAS-A β 42/+* (A β 42) were all raised at 18°C during development, then shifted to 29°C for 7–8 days after adult eclosion. Immunoblot analyses were performed for K_v4, and normalized to syn (Left). For quantitative analyses (Right), n = 4 for each condition, * P < 0.05, Student's t-test. (D) A β 42-induced decrease in K_v4 current is also absent by the genetic inhibition of the proteasome described in (C) (right). *elav-GAL4;UAS-Pros26¹/UAS-A β 42;UAS-Pros β ²/+* and *elav-GAL4;UAS-Pros26¹/+;UAS-Pros β ²/+* flies were raised at 18°C during development, then shifted as newly-eclosed adult flies to 29°C for 7–8 days (n = 4 for immunoblots, and n = 8 for each current recordings). Scale bars represent 25 pA and 50 ms. (E) Representative K_v4 and K_v2–3 currents in Ctrl and *elav-GAL4;UAS-A β 42* (A β 42) neurons from cultures treated with 20 μ M leupeptin for 8 days. 20 μ M leupeptin blocked the A β 42-induced decrease in K_v4 current density seen in Ctrl neurons.

doi:10.1371/journal.pgen.1005025.g004

in A β 42-neurons. These results suggest that the lysosome, in addition to the proteasome, is involved in A β 42-induced K_v4 degradation.

Transgenic Restoration of K_v4 Rescues Hyperexcitability

To test whether we could restore A β 42-induced hyperexcitability, we generated transgenic lines over-expressing *UAS-K_v4* in A β 42-expressing animals. More than 10 *UAS-K_v4* lines were isolated with different insertion sites of the transgene; each line was crossed to an *elav-GAL4*

driver and expression levels were tested by immunoblot analysis. We selected lines that raised K_v4 protein levels and K_v4 current amplitudes in Aβ42-expressing heads to near wild-type levels (Fig. 5A-B); we refer to these as Aβ42+ K_v4 neurons (*elav-GAL4;UAS-Aβ42/UAS-K_{v4}*). We then performed current-clamp recordings to determine if restoration of K_v4 reduced excitability in ramp stimulation protocols, as performed in Fig. 1A. We found that in Aβ42+ K_v4 neurons, the average current (and charge transfer) required to induce AP firing was significantly increased, compared to neurons from cultures expressing Aβ42 alone, and was quite similar to background control neurons (Fig. 5C-D). These results suggest that the decreased threshold for AP firing observed in Aβ42 neurons is indeed due to the loss of K_v4 channels. We then used these Aβ42+ K_v4 lines to test whether downstream cognitive and motor dysfunction would be attenuated.

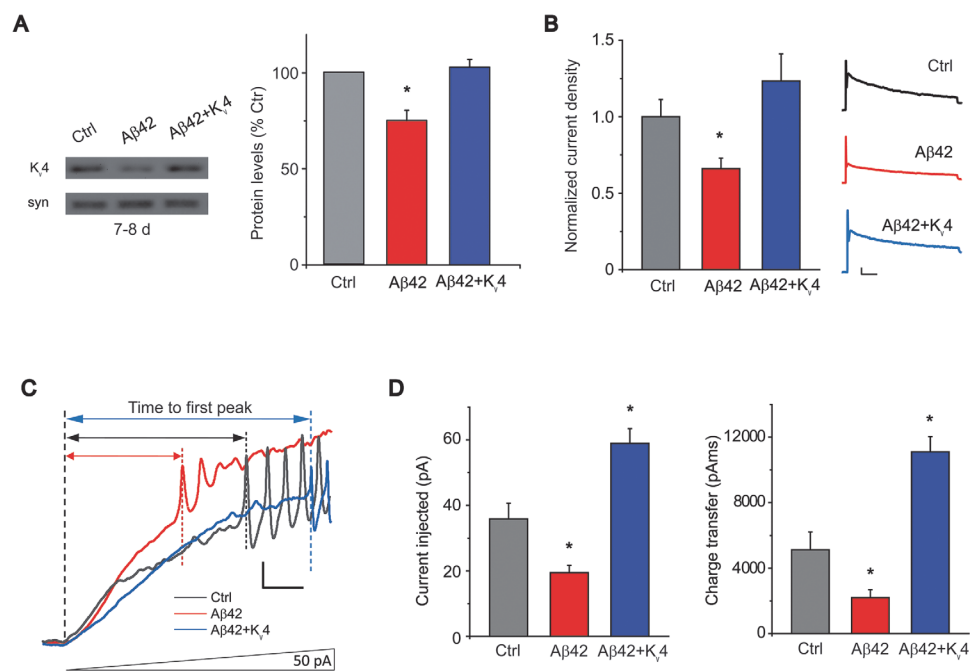


Fig 5. Transgenic over-expression of K_v4 in Aβ42-expressing flies restores K_v4 protein levels and normal excitability to neurons. (A) Immunoblot analyses of *UAS-Aβ42/+* (Ctrl), *elav-GAL4;UAS-Aβ42/+* (Aβ42), and *elav-GAL4;UAS-Aβ42/UAS-K_{v4}* (Aβ42 + K_v4) fly heads at 7–8 days are shown. Transgenic expression of *UAS-K_{v4}* restores K_v4 protein levels to wild type levels. ($n = 3$ for each group, * $P < 0.05$, Student's t test). (B) Representative K_v4 currents isolated in voltage-clamp mode from primary neurons, from cultures 9 days old, from Ctrl, Aβ42 and *elav-GAL4;UAS-Aβ42/UAS-K_{v4}* (Aβ42+ K_v4) flies are shown (Right). The K_v2 - K_v3 DR component was recorded using a prepulse of -45 mV to completely inactivate K_v4 channels, before stepping to a test potential of $+50$ mV; the K_v4 current was then isolated by subtracting this DR component from the total whole-cell current elicited from a prepulse of -125 mV, stepping to a test potential of $+50$ mV. Current density was obtained by dividing peak current amplitude by cell capacitance. Quantitative analyses (Left) show that K_v4 current density from Aβ42 neurons (194.3 ± 23.68 pA, $n = 9$) were significantly smaller than from Ctrl neurons (320.2 ± 33.52 pA, $n = 25$). K_v4 current density in Aβ42+ K_v4 neurons showed a near complete restoration (334.3 ± 48.97 pA, $n = 18$). * $P < 0.05$, Student's t -test. Scale bars represent 100 pA and 20 ms. (C) Representative current-clamp recordings from Aβ42 and the Aβ42+ K_v4 neurons in response to ramped stimulation protocol described in Fig. 1A, show that the time to first peak was significantly prolonged by the restoration of K_v4 to Aβ42-expressing neurons. Scale bar represents 10 mV and 50 ms. (D) Quantification of the average current injected and charge transfer required to elicit the first AP are shown. Both were significantly increased with transgenic restoration of K_v4 : 58.9 ± 4.54 pA, $n = 9$ (Left), and $11,108.0 \pm 920.49$ pAms, $n = 9$ (Right); note that quantification for Ctrl and Aβ42 values represent the same data set shown in Fig. 1B. * $P < 0.05$, Student's t -test.

doi:10.1371/journal.pgen.1005025.g005

Loss of K_v4 Plays a Critical Role in A β 42-Induced Learning Defects

We first investigated whether A β 42-induced loss of K_v4 would be predicted to affect learning in this fly model. We reasoned that the A β 42-induced changes observed in our aged late-embryonic cultures were likely to be relevant at larval stages. So, to examine learning, we used an odor-association learning assay with third instar larvae, similar to previously published studies [39]. Larvae were trained to associate a neutral odor (amyl acetate (AM), or 1-octanol (OCT)) with fructose, a natural appetitive attractant. In AM+/OCT- training, larvae were trained to associate AM with fructose, while in AM-/OCT+ training, larvae were trained to associate OCT with fructose (see [Materials and Methods](#)). After training, larvae were placed on a test plate with an AM source on one side, and an OCT source on the other side; after 20 minutes, the number of larvae on each half of the plate were counted. Standard preference scores (Pref) for AM and OCT were used to calculate a learning index (LI) for each independent pair of groups that had undergone AM+/OCT- and AM/OCT+ training (see [Materials and Methods](#)). We performed two sets of studies: first, to examine whether the loss of K_v4 function alone could lead to learning impairment, and second, to examine the effect of A β 42 on learning, and to determine if defects would be attenuated by K_v4 expression. Prior to these studies, we first confirmed that all genotypes showed a naïve preference for fructose ([S3A Fig.](#)), no preference for AM or OCT ([S3B Fig.](#)), and normal chemotaxis towards known attractants ([S3C Fig.](#)).

In the first set of studies, we tested whether the loss of K_v4 function alone would affect learning. To do this, we used a transgenic K_v4 dominant-negative line, *elav-GAL4;UAS-DNK_v4*, that completely eliminates K_v4 function [26]. We found that wild-type and the *UAS-DNK_v4* background stock performed similarly, showing a learned preference for the odor associated with fructose during training, with a LI of 0.43 +/- 0.08 and 0.48 +/- 0.05, respectively ([Fig. 6A](#)). In contrast, *elav-GAL4;UAS-DNK_v4* larvae showed no preference for either odor after training (LI = 0.06 +/- 0.15), similar to the known learning mutant *dunce* (*dnc*; LI = 0.08 +/- 0.11) ([Fig. 6A](#)). We further tested whether loss of K_v4 function in MBs alone affected learning/memory function. We used the MB driver *201y-GAL4* and found that in *201y-GAL4;UAS-DNK_v4* larvae, learning was also impaired (LI = 0.0 +/- 0.14; [Fig. 6A](#)), suggesting that K_v4 function in MBs is especially important for learning.

We next tested whether A β 42-expressing larvae display learning defects. We compared *elav-GAL4;UAS-A β 42/+* larvae with background control larvae containing either the *elav-GAL4* driver or the *UAS-A β 42* transgene alone. Larvae were trained, tested and scored as described above. We found that A β 42-expressing larvae exhibited a severely impaired LI, compared with background controls (LI = -0.03 +/- 0.09 for *elav-GAL4;UAS-A β 42/+*, LI = 0.23 +/- 0.08 for *UAS-A β 42/+*, $P < 0.05$; [Fig. 6A](#)). We then examined *elav-GAL4;UAS-A β 42/UAS-K_v4* larvae. We found that over-expression of K_v4 rescued learning defects in A β 42-expressing animals, restoring the LI to 0.29 +/- 0.06 ($p < 0.05$; [Fig. 6A](#)). Since all genotypes showed a similar naïve preference for fructose, no naïve preference for AM or OCT, and chemotaxis towards known attractants ([S3 Fig.](#)), no defects were likely due to impaired sensory transduction.

To test the specificity of the rescue of A β 42-induced learning defects by K_v4, we also expressed *UAS-K_v1*, *UAS-EKO*, or *UAS-CD8-GFP*, in A β 42-expressing flies. K_v1 (Shaker) is another A-type K⁺ channel in *Drosophila* that represents a multigene subfamily in mammals. EKO is a genetically modified *Drosophila* K_v1 channel. EKO channels have been altered so that their activation threshold is more hyperpolarized, near E_K, and their N-terminal inactivation mechanism has been disabled [40]; expression of EKO has been successfully used as a general suppressor of neuronal activity [40]. We found that the LI of *elav-GAL4;UAS-A β 42/+* larvae (LI = 0.03 +/- 0.09) was not improved in *elav-GAL4;UAS-A β 42/K_v1* or *elav-GAL4;UAS-A β 42/+;UAS-EKO/+* larvae (LI = 0.075 +/- 0.12 and 0.03 +/- 0.10, respectively; [Fig. 6A](#)). Expression of

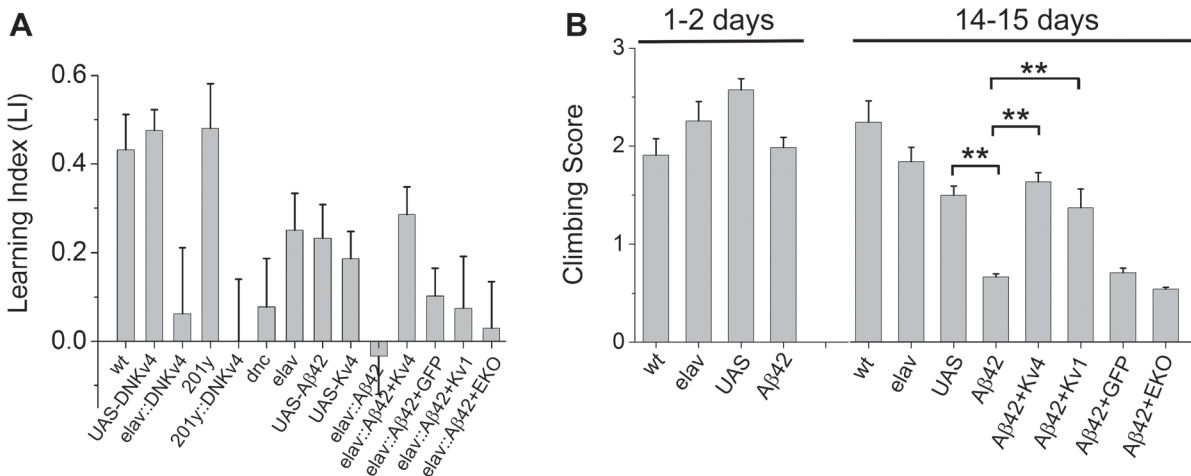


Fig 6. Larval olfactory associative learning and locomotion is defective in Aβ42-expressing larvae, and rescued by Kv4. (A) The following genotypes were trained and tested for learning function: wild-type (wt), *UAS-DNK_{v4}* (*UAS-DNK_{v4}*), *elav-GAL4;UAS-DNK_{v4}* (*elav-GAL4::DNK_{v4}*), *elav-GAL4* (*elav*), *UAS-Aβ42/+* (*UAS-Aβ42*), *UAS-K_{v4}* (*UAS-K_{v4}*), *elav-GAL4;UAS-Aβ42/+* (*elav::Aβ42*), *elav-GAL4;UAS-Aβ42/UAS-K_{v4}* (*elav::Aβ42+K_{v4}*), *elav-GAL4;UAS-Aβ42/UAS-K_{v1}* (*elav::Aβ42+K_{v1}*), *elav-GAL4;UAS-Aβ42/+;UAS-CD8-GFP* (*elav::Aβ42+GFP*), *elav-GAL4;UAS-Aβ42/+;UAS-EKO/+* (*elav::Aβ42+EKO*), *dnc¹* (*dnc*), *201y-GAL4* (*201y*), and *201y-GAL4;UAS-DNK_{v4}* (*201y::DNK_{v4}*). Learning was tested by training larvae to associate AM or OCT with fructose in the AM+/OCT- or AM-/OCT+ paradigms described in the text and Materials and Methods. After training, larvae were placed on a plain agarose test plate, with AM and OCT sources at opposite sides; after 20 minutes, larvae on each half of the plate were counted. Preference scores and a learning index (LI) were calculated, as described in Materials and Methods (*n* = 4–15 pairs of groups for each genotype, with one pair consisting of one group for AM+/OCT- training and one group for AM-/OCT+ training; 5 larvae per individual group). *elav-GAL4;UAS-DNK_{v4}*, *201y-GAL4;UAS-DNK_{v4}*, and *dnc* all showed significantly reduced learning indices, compared to wild-type and background controls. *elav-GAL4;UAS-Aβ42/+* also had a significantly reduced LI compared to background controls, which was rescued in *elav-GAL4;UAS-Aβ42/UAS-K_{v4}*, but not in *elav-GAL4;UAS-Aβ42/+;UAS-CD8-GFP/+*, *elav-GAL4;UAS-Aβ42/UAS-K_{v1}*, or *elav-GAL4;UAS-Aβ42/+;UAS-EKO/+*. (B) Locomotor activity was tested in a standard climbing assay on wild-type (wt), *elav-GAL4* (*elav*), *UAS-Aβ42/+* (*UAS*), *elav-GAL4;UAS-Aβ42/+* (*Aβ42*), *elav-GAL4;UAS-Aβ42/UAS-K_{v4}* (*Aβ42+K_{v4}*), *elav-GAL4;UAS-Aβ42/UAS-K_{v1}* (*Aβ42+K_{v1}*), *elav-GAL4;UAS-Aβ42/+;UAS-CD8-GFP/+* (*Aβ42+GFP*), and *elav-GAL4;UAS-Aβ42/+;UAS-EKO/+* (*Aβ42+EKO*) at 1–2 days and 14–15 days after eclosion, as described in text; each fly was given one point for every two tubes they climbed out of. The mean score of flies from each group (30–35 flies) was calculated; this was then repeated for 5–15 groups for each genotype with averages shown. *elav-GAL4;UAS-Aβ42/+* flies showed a significant impairment at 14–15 days, compared with *UAS-Aβ42/+* background controls. Co-expression of *UAS-K_{v4}* or *UAS-K_{v1}* rescues this impairment, while expression of *UAS-EKO* did not. * denotes *P* < 0.05, Student's t-test.

doi:10.1371/journal.pgen.1005025.g006

UAS-CD8-GFP, a non-channel transmembrane protein, also showed no rescue of Aβ42-induced learning defects (Fig. 6A). Thus, the rescue of Aβ42-induced learning defects by Kv4 appears to be specific, as it could not be replicated with Kv1 or EKO expression. In addition, these results show that expression of another *UAS* construct (*UAS-Kv1*, *UAS-EKO*, *UAS-CD8-GFP*) did not dilute the effect of *UAS-Aβ42* on learning. Altogether, these studies suggest that Aβ42-induced loss of Kv4 is likely to be a critical contributor to downstream learning defects.

Restoration of Kv4 Levels Rescues Locomotor Defects

Aβ42 expression has previously been shown to result in age-dependent climbing defects [16,18]. Interestingly, we have previously shown that loss of Kv4 function in *elav::UAS-DNK_{v4}* flies results in over-excitation of neurons, loss of reliable repetitive firing, and impaired repetitive behaviors, such as climbing [26]. One possibility is that the Aβ42-induced decrease in Kv4 contributes to the age-dependent locomotor deficit of Aβ42-expressing flies. So, we examined whether transgenic restoration of Kv4 was able to rescue the impaired locomotor function seen in Aβ42-expressing flies. Flies were collected over a 2 day period, then aged either 1 or 14 additional days. We used a standard assay that examines the ability of flies to climb against gravity [41,42]; flies' performance was scored as described (Materials and Methods). At 1–2 days AE, *elav-GAL4;UAS-Aβ42/+* flies scored similarly (1.98 +/- 0.11, *n* = 10) to background controls (2.25 +/- 0.20 for *elav-GAL4*, 2.57 +/- 0.11 for *UAS-Aβ42/+*, *n* = 10; Fig. 6B). In contrast, at

14–15 days AE, *elav-GAL4;UAS-A β 42/+* flies scored significantly lower (0.66 +/- 0.04, n = 10) than background control lines (1.84 +/- 0.15 for *elav-GAL4*, 1.49 +/- 0.09 for *UAS-A β 42/+*, n = 10; Fig. 6B), as expected. We then examined *elav-GAL4;UAS-A β 42/UAS-K $_v$ 4* flies at 14–15 days. We found that over-expression of K $_v$ 4 increased climbing scores to near wild-type levels (1.63 +/- 0.09, n = 10, $P < 0.01$; Fig. 6B). In contrast, expression of EKO channels or CD8-GFP did not significantly improve climbing scores (0.54 +/- 0.02, n = 10 or 0.71 +/- 0.05, n = 10, respectively; Fig. 6B). These results suggest that the A β 42-induced loss of K $_v$ 4 channels underlies downstream locomotor defects. Interestingly, over-expression of K $_v$ 1 also rescued the A β 42-induced climbing score (1.37 +/- 0.60, n = 10; Fig. 6B), suggesting that the A-type channel properties of K $_v$ 1 may be able to substitute for K $_v$ 4 function in locomotor activity.

Restoration of K $_v$ 4 Slows A β 42-Induced Neurodegeneration

We next investigated whether raising K $_v$ 4 levels in A β 42 neurons to near wild-type levels, as described above, would attenuate the age-dependent neuronal loss that has been reported to begin at 25 days AE [16]. While secreted A β 42, and K $_v$ 4, were over-expressed pan-neuronally, we assayed for cell loss specifically in the MBs, using the *GFP.S65T.T10* transgene. We counted GFP-labeled MB neurons from: 1) a background control line (*elav-GAL4*), 2) the A β 42-expressing line (*elav-GAL4;UAS-A β 42/+*), and 3) an A β 42+K $_v$ 4 line (*elav-GAL4;UAS-A β 42/UAS-K $_v$ 4*). GFP-labeled MB neurons in the intact brain were imaged by confocal microscopy, and cell bodies were counted from images taken at a fixed position (see Fig. 1A) at 15, 25, 40, and 50 days AE (aged at 22–23°C). As expected, cell numbers progressively decreased from 25 to 50 days in flies expressing A β 42 (Fig. 7A). In the A β 42+K $_v$ 4 line, however, the onset of cell loss was delayed, with no significant degeneration at 25 days (Fig. 7A); at 50 days, cell loss was attenuated by 58% (Fig. 7A). Expression of K $_v$ 4 in a wild-type background (*elav-GAL4;UAS-K $_v$ 4/+*) did not increase cell survival (Fig. 7A), suggesting that amelioration of neurodegeneration in A β 42+K $_v$ 4 brains was indeed due to the restoration of K $_v$ 4.

We also tested whether expression of A β 42 exclusively in MB neurons would induce local degeneration, and if so, whether this degeneration was also due to hyperactivity generated by the loss of K $_v$ 4. We used the MB GAL4 transgene, *201y-GAL4*, to drive expression of *UAS-A β 42*, with and without *UAS-K $_v$ 4*. In brains from 40 day old flies, we found that the number of MB neurons was reduced by ~17%, compared to brains from a background control line (Fig. 7B). When *UAS-K $_v$ 4* was co-expressed with *UAS-A β 42*, however, the number of MB cells were similar to controls (Fig. 7B). We also tested if expression of *UAS-EKO* would attenuate A β 42-induced MB degeneration. The *201y-GAL4* transgene was used to drive MB expression of *UAS-A β 42*, with and without *UAS-EKO*; flies were aged for 15 and 40 days, then GFP-labeled MB neurons were counted. We found that EKO did not slow A β 42-induced MB degeneration (Fig. 7B), suggesting that the loss of K $_v$ 4 function, in particular, plays a role in this neuronal degeneration.

To further examine the specificity of the role of K $_v$ 4 in A β 42-induced MB degeneration, we investigated the effect of expressing a general *UAS* construct, *UAS-GFP*, or the other A-type K $^+$ channel in *Drosophila*, *UAS-K $_v$ 1*. In addition, we used another method for quantifying MB neurons and co-labeled for A β 42 expression. We dissected brains from *elav;UAS-A β 42/+* flies with and without *UAS-K $_v$ 4*, *UAS-GFP*, or *UAS-K $_v$ 1* transgenes at 15, 25, and 40 days AE. Brains were co-labeled with DAPI to count cell bodies, and an anti-A β 42 antibody to compare levels of A β 42. Brains were imaged by confocal microscopy, as described above, and DAPI-positive cell density was quantified in the MB (Fig. 8A). No cell loss was seen at 15 days AE. Similar to our results quantifying GFP-positive MB cells, we detected a significant loss of DAPI-positive MB cells first at 25 days AE ($P < .01$), then continuing at 40 days AE ($P < 0.001$, Fig. 8B).

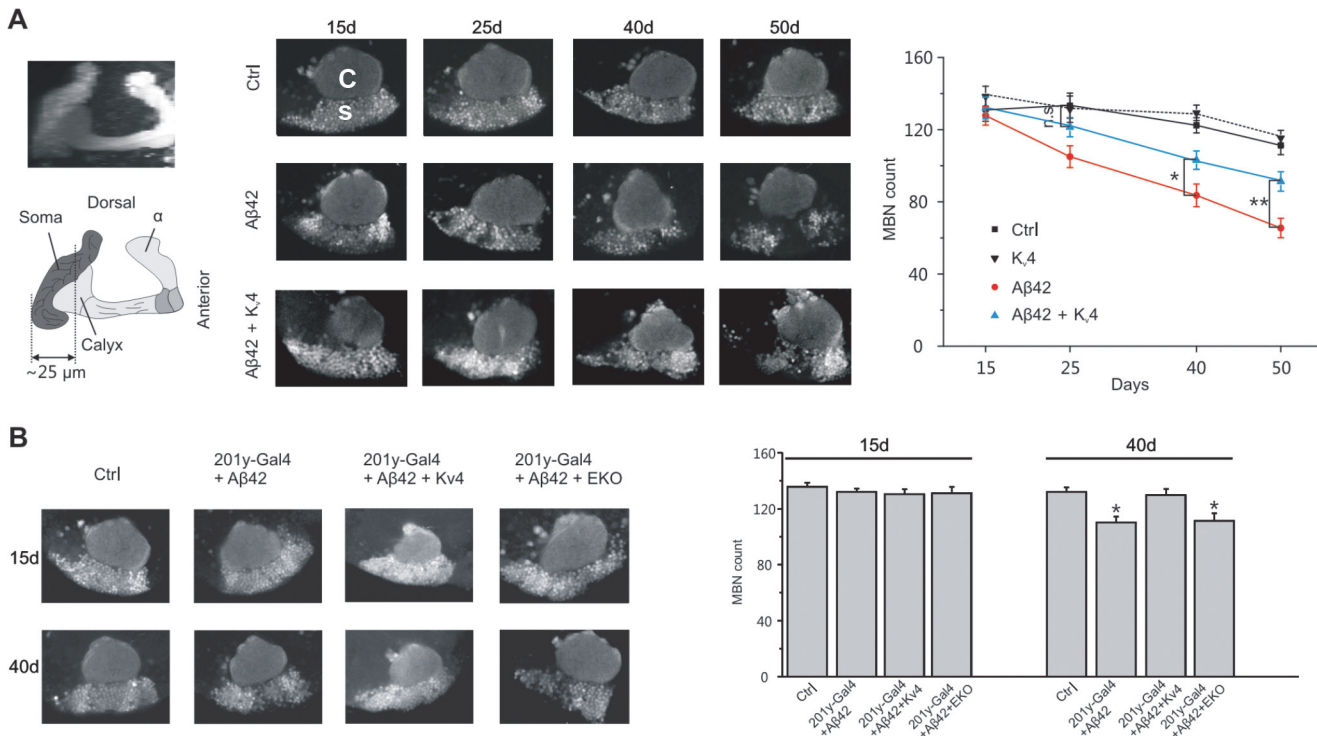


Fig 7. Restoration of excitability in Aβ42-expressing flies ameliorates age-dependent neuronal loss in MBs. (A) Converged confocal z-stack images of a typical mushroom body from the transgenic line, *elav-GAL4;;GFP.S65T.T10/+* (Left, Top), and a corresponding diagram with regions containing cell bodies, dendrites (in calyx), and axons shown (Left, bottom); MB neurons were GFP labeled by the *GFP.S65T.T10* transgene (regardless of GAL4 driver present, see text) and counted from single images taken 25 μm from the posterior-most edge of MB, as depicted by the dotted line shown. Representative confocal images used for counting neurons are shown from *elav-GAL4;;GFP.S65T.T10/+* (Ctrl), *elav-GAL4;UAS-K_v4/+;GFP.S65T.T10/+* (K_v4), *elav-GAL4;UAS-Aβ42/+;GFP.S65T.T10/+* (Aβ42), and *elav-GAL4;UAS-Aβ42/UAS-K_v4;GFP.S65T.T10/+* (Aβ42 + K_v4) flies at indicated ages: 15, 25, 40 and 50 days AE (Middle); in confocal images, the calyx (C) is seen above the region containing MB cell somas (s). Quantitative analyses show that restoration of normal excitability by transgenic *UAS-K_v4* expression significantly increases neuronal survival at 40 and 50 days, delaying the onset of neurodegeneration (no significant (n.s.) difference between Ctr and Aβ42 + K_v4 at 25 d) (Right). (n = 6–7 for each group, * P < 0.05, ** P < 0.01, Student's t-test). (B) Local expression of *UAS-Aβ42* was induced using the MB driver *201y-GAL4*. Representative confocal images and quantification, as described in (A), are shown from *201y-GAL4;GFP.S65T.T10/+* (Ctrl), *201y-GAL4/UAS-Aβ42/+;GFP.S65T.T10/+* (201y-Gal4+Aβ42), *201y-GAL4/UAS-Aβ42;GFP.S65T.T10/UAS-K_v4* (201y-Gal4+Aβ42+K_v4), and *201y-GAL4/UAS-Aβ42;UAS-EKO/GFP.S65T.T10* (201y-Gal4+Aβ42+EKO) heads at 15 and 40 days after eclosion. Local expression of Aβ42 results in a significant reduction in MBNs at 40 days (110.30 ± 4.03), compared to Ctr (132.10 ± 3.17), which is rescued by K_v4 expression (129.40 ± 4.18), but not expression of EKO (111.30 ± 4.76); n = 8–9 brains for each condition, *P < 0.05, Student's t-test.

doi:10.1371/journal.pgen.1005025.g007

Over-expression of K_v4 delayed the onset, and slowed, the ensuing degeneration (Fig. 8B). Since expression of *UAS-GFP* did not attenuate or slow the Aβ42-induced degeneration at 25 or 40 day AE (Fig. 8B), it is unlikely that inclusion of an additional *UAS* target site alone leads to decreased expression of Aβ42 and apparent rescue of neurodegeneration. Indeed, quantification of Aβ42 revealed no loss of Aβ42 expression in Aβ42+K_v4 MBs (Fig. 8C).

Interestingly, expression of *UAS-K_v1* resulted in increased cell survival in Aβ42-expressing animals at 25 days AE, but not at 40 days AE (Fig. 8B). These results suggest that A-type K⁺ channel function from K_v1 can help decrease the severity of initial degeneration, perhaps by ameliorating hyperexcitability. Also interestingly, we found that loss of K_v4 function alone did not induce neurodegeneration, as observed by DAPI-positive MB cell density in *elav;;UAS-DNK_v4* compared to a background control line at 25 and 40 days AE (Fig. 9). Altogether our results suggest that while the loss of K_v4 channels, and ensuing hyperexcitability, are key factors that exacerbate neurodegeneration, the Aβ42-induced reduction of K_v4 channels is not sufficient to trigger degeneration.

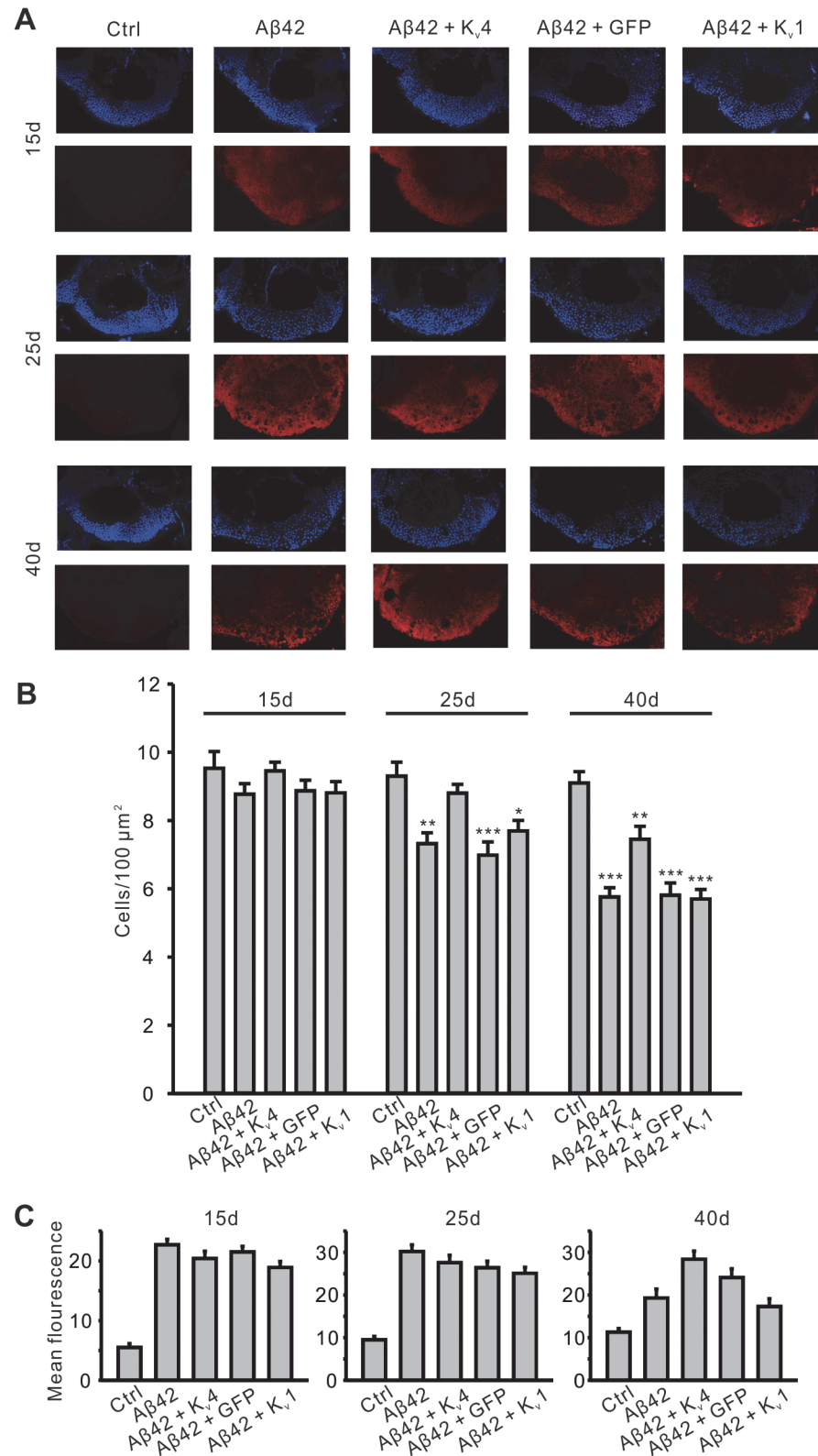


Fig 8. Pan-neuronal expression of K $_v$ 4 slows the onset and severity of A β 42-induced neurodegeneration. (A) Representative confocal images, from MB position described in Fig. 7, show nuclear (DAPI) staining (upper panels, blue) from five genotypes, including *UAS-A β 42/+* (Ctrl), *elav-GAL4;UAS-A β 42/+*

(Aβ42), *elav-GAL4;UAS-Aβ42/UAS-K_v4* (Aβ42+K_v4), *elav-GAL4;UAS-Aβ42/UAS-GFP* (Aβ42+GFP) and *elav-GAL4;UAS-Aβ42/UAS-K_v1* (Aβ42+K_v1). Co-immunolabeling for Aβ42 is shown (lower panels, red) from these genotypes. Brains were dissected and labeled from flies aged 15 days (15d), 25 days (25d) and 40 days (40d) AE. Note that Aβ42 immunostaining is clearly seen in all the genotypes except Ctr. (B) Quantification of cell density (DAPI-positive) from confocal images described in (A). Note that there is significant cell loss in Aβ42, Aβ42+GFP, and Aβ42+K_v1 flies at 25d, but not in Aβ42+K_v4. n = 6–8 for each genotype, * P < 0.05, ** P < 0.01, *** P < 0.001, Student's t-test. (C) Relative anti-Aβ42 signal was quantified in the same aged genotypes described in (A); background fluorescence is reflected in Ctr samples. Note that no significant difference in Aβ42 signal was seen in Aβ42+K_v4 brains, compared to Aβ42 at 15 and 25 days AE; at 40d AE, Aβ42+K_v4 brains show an increase in Aβ42 signal; quantification, however, was difficult due to the number of degenerative “holes” seen in confocal sections at this age. n = 6–8 for each genotype. All data are expressed as means ± SEM.

doi:10.1371/journal.pgen.1005025.g008

Aβ42-Induced Loss of K_v4 Contributes to Premature Death

Since *elav-GAL4;UAS-Aβ42/+* flies have been shown to exhibit a shortened lifespan [16–18], we examined whether hyperactivity, generated by the loss of K_v4, might also contribute to this phenotype. We first examined whether loss of K_v4 function alone would affect lifespan. We compared two different insertions of *UAS-DNK_v4* (#14 and #20), and found that *elav-GAL4;UAS-DNK_v4* survivorship was significantly decreased, with a median age of 31 and 47 days, compared to 67 and 82 for respective controls ($P < 0.0001$ by log-rank analyses; Fig. 10A). We then restricted expression of *UAS-DNK_v4* to the adult to eliminate effects from loss of K_v4 function during development. To do this, we used the *UAS-GAL4-GAL80^{ts}* system [43] to induce expression of *UAS-Aβ42* in the nervous system only after adult eclosion. In this system, the GAL80 protein inhibits GAL4 function and therefore Aβ42 expression. We used the *tub-GAL80^{ts}* transgene, which expresses a temperature-sensitive GAL80^{ts} protein under the control of the tubulin promoter; at 18°C, the GAL80^{ts} protein is functional, while a shift to 30°C renders the GAL80^{ts} protein non-functional. Flies containing *elav-GAL4*, *tub-GAL80^{ts}*, and *UAS-DNK_v4* transgenes (*elav-GAL4;tub-GAL80^{ts};UAS-DNK_v4*) were raised at 18°C to prevent expression of *UAS-DNK_v4*, then shifted to 30°C to induce expression of DNK_v4 for the lifespan of the adults. Longevity of *elav-GAL4;tub-GAL80^{ts};UAS-DNK_v4* flies was significantly shorter (median age of 32 days; $p < 0.0001$) than wild-type (median age of 39 days) and background control (median age of 37 days) lines under similar conditions (Fig. 10B). These results suggest that K_v4 function in the adult is likely to play a role in longevity.

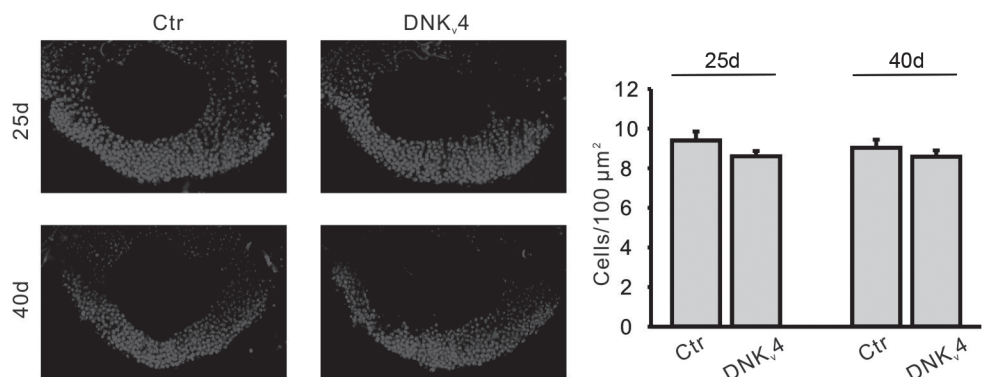


Fig 9. No significant MB cell loss is found in the DNK_v4 transgenic line. Representative images (Left) and quantification (Right) of nuclear (DAPI) staining in MBs of *UAS-DNK_v4* (Ctr) and *elav-GAL4;UAS-DNK_v4* (DNK_v4) at 25 and 40 days AE. MB orientation and position of confocal image as described in Fig. 7. No significant difference in cell density was seen in DNK_v4 brains compared to controls. n = 6 for each genotype. Data are expressed as means ± SEM.

doi:10.1371/journal.pgen.1005025.g009

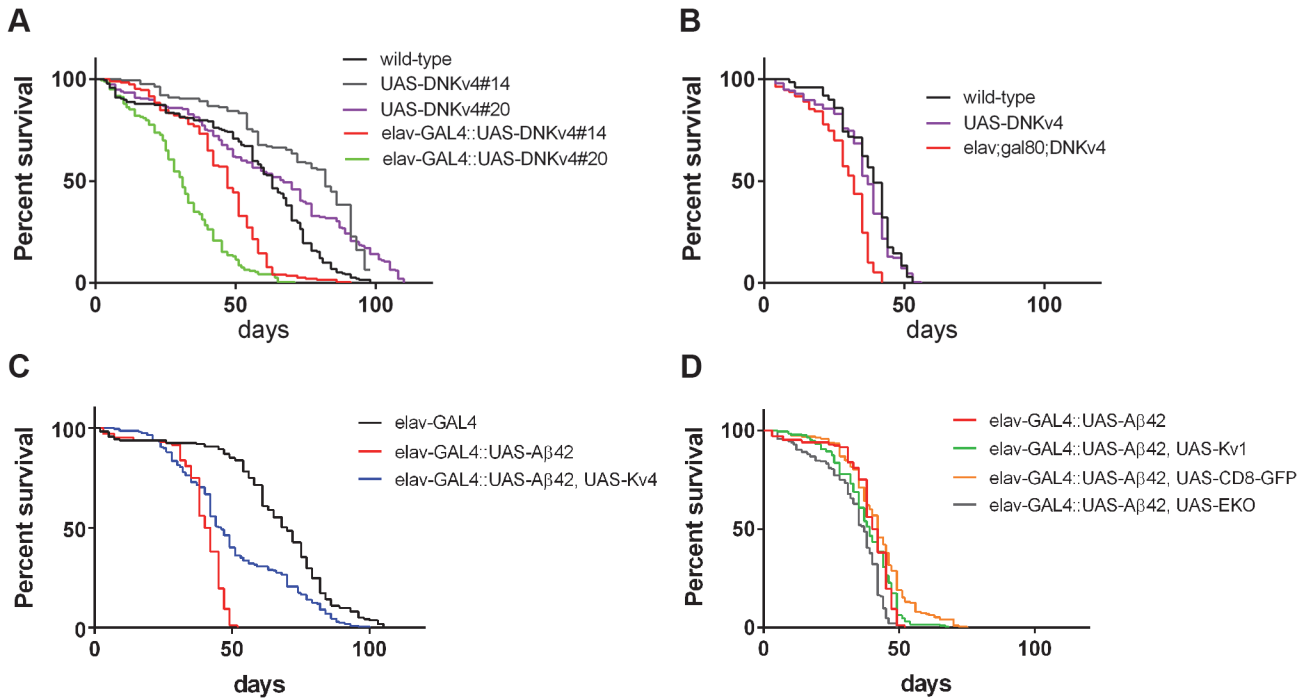


Fig 10. Premature death is partially rescued by expression of *Kv4* in A β 42-expressing flies. (A-D) Longevity assays, using populations of ~200 male flies, for indicated genotypes (see [Materials and Methods](#)). (A) Survival plots for wild-type, two different transgenic insertions of *UAS-DNKv4* (#14 and #20), and *elav-GAL4::UAS-DNKv4* (*elav-GAL4::UAS-DNKv4*) lines are shown. Neuronal expression of *UAS-DNKv4* leads to a significantly reduced ($P < 0.0001$ by log-rank analyses) lifespan at 25°C compared to *UAS* background controls. (B) Longevity assays performed for flies raised at 18°C during development, then shifted to 30°C for the entirety of the adult lifespan. Induced expression of *DNKv4* resulted in a significantly reduced lifespan (*elav-GAL4;tub-GAL80ts;UAS-DNKv4*; median age of 32 days), compared to wild-type (median age of 39 days) and *UAS-DNKv4* (median age of 37 days); significance of $P < 0.0001$ by log-rank analyses. (C-D) Survival plots for *elav-GAL4*;+ (*elav-GAL4*), *elav-GAL4;UAS-A β 42*/+ (*elav-GAL4::UASA β 42*), *elav-GAL4;UAS-A β 42/UAS-Kv4* (*elav-GAL4::UASA β 42,UAS-Kv4*), *elav-GAL4;UAS-A β 42/UAS-Kv1* (*elav-GAL4::UASA β 42,UAS-Kv1*), *elav-GAL4;UAS-A β 42/+;UAS-CD8-GFP/+* (*elav-GAL4::UASA β 42,UAS-CD8GFP*), and *elav-GAL4;UAS-A β 42/+;UAS-EKO/+* (*elav-GAL4::UASA β 42,UAS-EKO*); all of these assays were performed at 25°C. *elav-GAL4;UAS-A β 42*/+ flies show a severely reduced lifespan (median age of 41 days) at 25°C, compared with the *UAS-A β 42*/+ background control (median age of 70 days; significance of $P < 0.0001$ by log-rank analyses). *elav-GAL4;UAS-A β 42/UAS-Kv4* flies showed a partial rescue of lifespan (median age of 46 days; $P < 0.0001$ by log-rank and Gehan-Breslow-Wilcoxon analyses), while *elav-GAL4;UAS-A β 42/+;UAS-EKO/+*, *elav-GAL4;UAS-A β 42/Kv1*, and *elav-GAL4;UAS-A β 42/+;UAS-CD8-GFP/+* flies did not show a significant improvement in lifespan from *elav-GAL4;UAS-A β 42*/+ flies.

doi:10.1371/journal.pgen.1005025.g010

We next compared the longevity of *elav-GAL4;UAS-A β 42*/+ flies with background control lines. We found that *elav-GAL4;UAS-A β 42*/+ flies have a greatly shortened lifespan (median age of 41 days) compared to the control line (median age of 70 days, $p < 0.0001$; [Fig. 10C](#)). We then tested *elav-GAL4;UAS-A β 42/UAS-Kv4* flies to see if restoration of normal excitability would attenuate premature death induced by A β 42. Over-expression of *Kv4* in A β 42-expressing flies resulted in a small, but significant, increase in lifespan (median age of 46 days, $p < 0.05$; [Fig. 10C](#)). Over-expression of *Kv1*, *EKO*, or *CD8-GFP*, however, did not significantly increase the lifespan of A β 42-expressing flies (median ages of 37, 39, and 42 days, respectively; [Fig. 10D](#)). These results further support the partial, yet specific, rescue of premature death by *Kv4* expression.

Discussion

A β -induced hyperexcitability is indeed intriguing, with interesting implications especially for seizure-like activity and epilepsy, which are potentially associated with AD [11,15,44,45]. Little, however, has been done previously to determine whether A β -induced hyperactivity contributes to downstream behavioral pathologies. Recent studies, however, have suggested that neuronal

hyperactivity may precede neurological dysfunction [46] and may be improved by pharmacologically reducing activity [44]. In this study, we show, in cultured neurons and in the intact brain, that K_v4 channels are specifically down-regulated by A β 42 expression, while other K⁺ currents (eg. K_v2 and K_v3) remain unaltered. The resulting increase in neuronal excitability was present in the adult brain at an age (8 days AE) before the appearance of locomotor (14–15 days AE) and learning defects (14 days AE; ref), and before the onset of neurodegeneration (25 days AE), supporting the hypothesis that hyperactivity precedes and contributes to these downstream pathologies. We then show that increasing K_v4 channel levels in A β -expressing animals restores normal excitability to neurons, and as a result, completely rescues learning and locomotor defects, slows neurodegeneration, and slightly increases lifespan. It is significant to note that the expression of a *UAS-GFP* or *UAS-CD8-GFP* transgene did not rescue any of these pathologies, suggesting that any rescue effects by *UAS-K_v4* were not simply due to the introduction of another *UAS* target for GAL4 that would dilute the expression of A β 42; indeed, quantification of A β 42 was not any lower in A β 42+K_v4 flies. In future studies, it will be interesting to examine the temporal requirement for reducing excitability with K_v4 expression; for example, is early hyperexcitability more “toxic” to the system than later stage hyperexcitability?

Although specificity of rescue by K_v4 varied from one pathology to another, the genetically engineered EKO channel that acts as a general activity inhibitor did not ameliorate any of the cognitive, motor, or survival deficits tested. This suggests that general dampening of excitability was not sufficient to replace K_v4 loss. K_v1, the other A-type K⁺ channel present in *Drosophila*, however, was able to rescue A β 42-induced locomotor dysfunction, but, interestingly, not learning or premature death. These results are consistent with the fact that K_v1 and K_v4 share some, but certainly not all, biophysical properties. For example, K_v4 channels have a much more hyperpolarized voltage-operating range than K_v1 channels, making them much more likely to play roles at subthreshold potentials [20,21]. Also, while both K_v4 and K_v1 channels display fast inactivation, the inactivation rate is voltage-independent for K_v4 channels and voltage-dependent for K_v1 channels [20,21]. Finally, the subcellular localization of K_v4 and K_v1 channels are thought to be distinct, with K_v4 channels restricted to dendrites and cell bodies, and K_v1 channels localized in axons and nerve terminals.

We also examined whether the loss of K_v4 function alone was sufficient to lead to cognitive and motor pathologies. Previously, we had shown that expression of a dominant-negative K_v4 subunit, DNK_v4, results in the elimination of the K_v4 current [26]. Loss of K_v4 function led to increased excitability and locomotor deficits [26,47,48]. In the present study, we found that expression of DNK_v4 also induced learning defects and a shortened lifespan, consistent with a key role for the A β 42-induced reduction in K_v4 in these downstream pathologies. In mammalian systems, K_v4.2 has been shown to play a role in the induction of long-term potentiation (LTP) [49], and hippocampal dependent learning/memory defects [50]. Loss of K_v4 function alone, however, did not induce any significant neurodegeneration, suggesting that while A β 42-induced loss of K_v4 exacerbates degeneration, it is not sufficient to trigger neurodegenerative pathway(s).

Previous reports over the years have shown different effects of A β on A-type K⁺ currents *in vitro*, with some identifying decreases in I_A [51,52] and others reporting increases in I_A [4,53–57]. Differences between these studies are likely to be due to a variety of factors including the species of A β tested (eg. A β 1–40, A β 1–42, A β 25–35; some studies finding clear differences with different A β species [56], the cell type examined (eg. HEK cells, hippocampal neurons, or cortical neurons), and the time course of the effect (eg. from seconds to days in different studies). For example, the A β species applied, the concentration used, and time incubated with cells all affect the assembly state of A β , which has also been proposed to have differential downstream effects on K⁺ currents [4,51] and excitability/activity [8,12]. In the future, it will be interesting

to see how effects on K_v4 develop, and possibly change, throughout the assembly of A β 42 from monomers to oligomers, protofibrils, and mature fibrils *in vivo*.

Much remains to be understood about the mechanism by which K_v4 channels are lost in response to A β 42 expression. In this study, pharmacological and genetic approaches suggest a degradation pathway for K_v4 that depends on both the proteasome and lysosome, similar to the EGF receptor [35,36]. This scenario is likely to be complicated since previous studies have shown that A β directly inhibits the proteasome [58], and that clearance of A β depends on the proteasome [59–62]. Further study is needed to understand how K_v4 channels are targeted for turnover by A β 42, and what other component(s) are involved.

Further study is also needed to unravel specific mechanisms by which K_v4 channels function in downstream A β 42 pathologies. For example, how does the loss of K_v4 exacerbate neurodegeneration? One possibility is that cell death is induced by an “excitotoxic” pathway due to excess Ca²⁺ entry, and ultimately, necrosis. Interestingly, previous studies have shown that A β 42 induces an increase in various K⁺ currents that are linked to cell death *in vitro* [63–65], consistent with evidence that efflux of K⁺ is required as an early step in apoptosis [66]. While it is not clear how to reconcile these findings with ours, it does seem that proper K⁺ homeostasis is critical for neuronal survival. The role of K_v4 in lifespan, however, is complex, given that neurodegeneration, learning/memory formation, and locomotor activity all contribute to survival. The partial to full rescue of multiple A β 42-induced pathologies by K_v4, however, underscores the importance of the loss of K_v4 *in vivo* and suggests that K_v4 is a critical target of A β 42 in this model, and perhaps in AD.

Materials and Methods

Fly Stocks

We used previously generated transgenic lines: *UAS-GFP-K_v4* [67,68], *UAS-A β 40* and *UAS-A β 42/CyO* [16–18], *GFP.S65T.T10* [30,31], *UAS-Pros26¹;UAS-Pros β ²* [32], and *UAS-EKO* [40]. For *UAS-K_v4*, the wild-type *Shal2* isoform was subcloned into the *pENTR1A* vector (Gateway pENTR vectors, Invitrogen), then recombined *in vitro* using lambda integrase into the *pTW* destination vector (*Drosophila* Gateway Vector Collection, available through the *Drosophila* Genomics Resource Center), generating the *pUAST-Shal2* transformation vector. Microinjection with transposase into *w¹¹¹⁸* embryos to generate transgenic lines was performed by Rainbow Transgenics (Camarillo, CA), then mapped and balanced by standard procedures. For behavioral studies, fly lines were successively outcrossed at least five times before use.

Whole-Brain and Embryonic Neuronal Cultures

For whole-brain cultures, flies (2 days after eclosion) were anaesthetized, and the brains were quickly dissected, as reported previously [25]. We incubated the cultures in a humidified chamber at room temperature and refreshed the culture medium (18% fetal bovine serum, 100 U/mL penicillin, 100 μ g/mL streptomycin in Schneider’s *Drosophila* culture medium) every 12 hours. 10 brains were sonicated for each immunoblot sample. For embryonic neuronal cultures, single embryos aged 5–6 hours (at room temperature) were dissociated in 20 μ L drops of culture medium, as previously described [20,21,25].

Electrophysiology

Whole-cell recordings were performed in perforated patch-clamp configuration by adding 400–800 μ g/ml Amphotericin-B (Sigma-Aldrich) in the pipette, as reported previously [25,26]. For current-clamp recordings, we used external solution (in mM): NaCl, 140; KCl, 2; HEPES, 5;

CaCl₂, 1.5; MgCl₂, 6, with pH 7.2. For K⁺ current recordings in cultured MB neurons, we used external solution (in mM): Choline-Cl, 140; KCl, 2; MgCl₂, 6; HEPES, 5, with pH 7.2. For K⁺ current recordings from GFP-labeled MB neurons in the intact brain, we exchanged culture medium to the external solution (in mM): NaCl, 110; KCl, 2; MgCl₂, 6; glucose, 5; NaHCO₃, 20; NaH₂PO₄. Solution was continuously bubbled with carbogen (5% oxygen and 95% carbon dioxide) throughout recording; pH was set at 7.2. TTX (1 μ M) and nifedipine (10 μ M) were added to the external solution to block Na⁺ and Ca²⁺ currents. Electrodes were filled with internal solution (in mM): K-gluconate, 120; KCl, 20; HEPES, 10; EGTA, 1.1; MgCl₂, 2; CaCl₂, 0.1, with pH 7.2. We performed all recordings at room temperature. Electrode resistances for all recordings were 5–10 M Ω . Gigaohm seals were obtained for whole-cell recordings.

For analyses shown in Fig. 1D, the correlation coefficient (CC) between the membrane potential and the latency to the first AP was examined. Calculation of this CC was performed as a Pearson product-moment correlation coefficient. The CC is defined by $CC = S_{XY} / \sigma_X \sigma_Y$, where σ_X and σ_Y are the standard deviations (SDs) of the samples, and S_{XY} is the sample covariance of X and Y. Here, X and Y represent the membrane potential and AP latency. The CC for membrane potential and AP latency in wild-type and A β 42 neurons were quantified, similar to a previous study [69].

Imaging and Immunoblot Analyses

For fly brain imaging, adult brains were dissected in phosphate buffer (0.1 M, pH 7.2), and fixed for 20 min in 4% paraformaldehyde, as previously described [67]. The isolated brains were washed in phosphate buffer for 5 min, 4 times. We either mounted the brains on the coverslips and captured the images on the same day (for pan-neuronal expression of A β 42), or blocked in 5% goat serum for 1 hour and immunolabeled with anti-GFP (1:1000) or Anti-A β 42 (Anti- β -Amyloid (1–42) Rabbit pAb, Calbiochem) in PBST at 4°C overnight (for experiments using the *201y-GAL4* driver). Brains were washed in PBST (5 min, 4 times) and then incubated with secondary antibody for 1 hour at room temperature; brains were washed (5 min, 4 times), then mounted (with DAPI) and imaged. Images were obtained using a Zeiss LSM 510 confocal microscope; images were processed and analyzed using Photoshop CS2 and Volocity v.6 software (Perkin Elmer).

Neuronal and A β 42 quantification. The number of GFP-labeled MB cells and DAPI-labeled cells at MB area were blindly counted by three independent investigators. To quantitate cell density, we chose regions of interest (ROIs) in the area of MB cell bodies of $\sim 400 \mu\text{m}^2$, and used 3 ROIs from each confocal image. For A β 42 quantification, grey values of labelled anti-A β 42 were determined after subtracting the background values, which were taken from non-immunostained brain images. Commonly, the MB area (cell bodies) $1200 \mu\text{m}^2$ in a single section (one from half brain, and two from the whole brain) were picked up for data collection and all data were pooled from around 6–8 brains for each genotype.

For immunoblot analyses, we used primary antibodies at the indicated concentrations, overnight at 21–23°C: anti-K_v4 (1:100; [68]), anti-syntaxin (1:100; 8C3 from Developmental Studies Hybridoma Bank, University of Iowa).

RT-PCR

Flies were collected, aged at 25°C, and stored at -80°C until ready to extract total RNA. TRI-ZOL RNA isolation procedure (Invitrogen/Life Science) was used to extract total RNA following homogenization of liquid nitrogen chilled flies in 1.5 ml RNase/DNase-free Eppendorf tubes with 1.5 ml RNase/DNase-free pestle (KONTES-Kimble Chase LLC). The quantity and quality of total RNA was analyzed by NanoDrop, and agarose gel electrophoresis. To eliminate

genomic DNA, RNA samples were treated with DNase I. DNase I treated RNA (1 μ g) was used as a template to synthesize first-strand cDNA by Superscript II RT (Invitrogen/ Life Science). K ν 4 specific primers were used for standard PCR. Sense primer: AGA ACG GGG ATC AGA ATC TGC A, anti-sense primer: CGG TGG CAA AGA TGA TAA TGG. The quantity of cDNA was measured by Image J following agarose gel electrophoresis. Quantification was averaged over three different total RNA extracts.

Learning/Memory Assays

Larvae were trained in groups of 5. In each training cycle, larvae were: 1) transferred to an “association plate” in which one of the odors is paired with an agarose-fructose (FRU) substrate for one minute, 2) moved to an agarose-only rest plate one minute, 3) moved to an agarose-only plate with the second odor, and 4) moved to an agarose-only rest plate; 10 such training cycles were performed. After training, larvae were placed on an agarose-only test plate with an AM source on one side, and an OCT source on the other side; after 20 minutes, the number of larvae on each half of the plate were counted. 5–15 groups were assayed for each genotype. Standard preference scores and learning indices were calculated as described in [39]. As an example, the preference score for AM (PREF_{AM}), and the learning index (LI) were calculated as shown:

$$\text{PREF}_{\text{AM}} = (\text{number of larvae}_{\text{AM}} - \text{number of larvae}_{\text{OCT}}) / \text{number of larvae}_{\text{TOTAL}}$$

$$\text{LI} = (\text{PREF}_{\text{AM+}/\text{OCT-}} - \text{PREF}_{\text{AM-}/\text{OCT+}}) / 2$$

Given: number of larvae_{AM} or larvae_{OCT} indicates the number of larvae on the AM or OCT, half or the test plate, respectively; PREF_{AM+}/OCT-} or PREF_{AM-}/OCT+} indicates the preference scores after either AM+}/OCT- or AM-}/OCT+ training, respectively.

Locomotion Assays

30–35 males in a 12.4 cm tall tube were allowed to climb upwards for 30 seconds into a second tube inverted on top of the first. The flies that successfully climbed into the second tube were given 30 seconds to climb from the bottom of the tube into a third tube. This process was continued through ten successive tubes and measured by a countercurrent distribution [41]; each fly was given a score of 0.5 for each tube that it climbed out of, similar to [42]. 5–15 assays, with ~30–35 naïve flies, were performed for each genotype tested.

Lifespan Analyses

For each genotype, a total population of 200 newly-eclosed male flies were collected and housed in food vials (10 flies/vial) at the indicated temperatures. Food vials were changed every 2–3 days and the number of dead/surviving flies was counted during each change. Log-rank statistical analyses were performed using GraphPad Prism 6 (GraphPad Software, Inc., La Jolla, CA).

Supporting Information

S1 Fig. Summarized results showing the I_A and delayed rectifier (DR) currents that are encoded by K ν 4 and K ν 2–3, respectively, from elav-GAL4 (Ctr) and elav-GAL4::UAS-A β 42/+ (A β 42). n = 8. Related to Fig. 2.

(TIF)

S2 Fig. Representative blots and quantification of K ν 4 protein levels from elav-GAL4 (Ctr2) and elav-GAL4::UAS-A β 42 (A β 42) heads at indicated ages. Related to Fig. 3.

(TIF)

S3 Fig. Olfactory and gustatory assays for genotypes used in learning assays. The following genotypes were tested: wild-type (wt), *UAS-DNK_v4* (*UAS-DNK_v4*), *elav-GAL4::DNK_v4* (*elav-GAL4::DNK_v4*), *elav-GAL4* (*elav*), *UAS-A β 42/+* (*UAS-A β 42*), *UAS-K_v4* (*UAS-K_v4*), *elav-GAL4::UAS-A β 42/+* (*elav::A β 42*), *elav-GAL4::UAS-A β 42/+;UAS-K_v4* (*elav::A β 42,K_v4*), *dnc¹* (*dnc*), *201y-GAL4* (*201y*), and *201y-GAL4::UAS-DNK_v4* (*201y::DNK_v4*). Related to Fig. 6. (A) All genotypes were tested for a natural preference for fructose by placing groups of 5–10 larvae in the center of circular plates with half plain agarose (1%) on one side, and half agarose (1%) + fructose (2M) on the other; after 20 minutes, larvae on each side of the plate were counted and preference scores calculated ($n = 3–5$ groups for each genotype). All showed a positive preference score for fructose. (B) Larvae were tested for a naïve olfactory preference for AM or OCT, on either plain agarose (AGAR) or agarose+fructose (FRUCTOSE), by placing groups of 5–10 larvae in the center of plates with AM and OCT sources at opposite sides ($n = 3–5$ groups were used); after 20 minutes, larvae were counted and preference scores calculated for AM/OCT. No genotype showed a strong preference for either odor on plain agarose or fructose. (C) To ensure that larvae could indeed smell, all genotypes were tested as in (B) with a natural attractant (methylacetate or acetone) on one side of the test plate and an empty source at the other. All genotypes showed a positive preference score for the attractants after 20 minutes ($n = 3–5$ groups of 5–10 larvae). (TIF)

Acknowledgments

We thank Drs. K. Iijima and Y. Zhong for the *UAS-A β 42* lines, Dr. M. Konsolaki for the *UAS-A β 40* line, Dr. W. Joiner for the *UAS-K_v1* lines, the Bloomington *Drosophila* Stock Center for the *UAS-EKO* line and Dr. T. Holmes for helpful assistance with its use. We also thank Dr. F. Diao for generating the *UAS-Shal2* transformation vector. We also thank Drs. Lin He and Long Cui for advice and training with confocal and quantification methods.

Author Contributions

Conceived and designed the experiments: YP ETH GW QS ST. Performed the experiments: YP ETH GW QS ST DAVB AL HB LG KF. Analyzed the data: YP ETH GW QS ST. Contributed reagents/materials/analysis tools: YP ST. Wrote the paper: YP ETH GW ST.

References

1. Glenner GG, Wong CW (1984) Alzheimer's disease: initial report of the purification and characterization of a novel cerebrovascular amyloid protein. *Biochem Biophys Res Commun* 120: 885–890. PMID: [6375662](#)
2. Tanzi RE, Bertram L (2005) Twenty years of the Alzheimer's disease amyloid hypothesis: a genetic perspective. *Cell* 120: 545–555. PMID: [15734686](#)
3. Walsh DM, Selkoe DJ (2004) Deciphering the molecular basis of memory failure in Alzheimer's disease. *Neuron* 44: 181–193. PMID: [15450169](#)
4. Ramsden M, Plant LD, Webster NJ, Vaughan PF, Henderson Z, et al. (2001) Differential effects of unaggregated and aggregated amyloid beta protein (1–40) on K(+) channel currents in primary cultures of rat cerebellar granule and cortical neurones. *J Neurochem* 79: 699–712. PMID: [11701773](#)
5. Hsieh H, Boehm J, Sato C, Iwatsubo T, Tomita T, et al. (2006) AMPAR removal underlies Abeta-induced synaptic depression and dendritic spine loss. *Neuron* 52: 831–843. PMID: [17145504](#)
6. Kamenetz F, Tomita T, Hsieh H, Seabrook G, Borchelt D, et al. (2003) APP processing and synaptic function. *Neuron* 37: 925–937. PMID: [12670422](#)
7. Palop JJ, Chin J, Roberson ED, Wang J, Thwin MT, et al. (2007) Aberrant excitatory neuronal activity and compensatory remodeling of inhibitory hippocampal circuits in mouse models of Alzheimer's disease. *Neuron* 55: 697–711. PMID: [17785178](#)

8. Busche MA, Chen X, Henning HA, Reichwald J, Staufenbiel M, et al. (2012) Critical role of soluble amyloid-beta for early hippocampal hyperactivity in a mouse model of Alzheimer's disease. *Proc Natl Acad Sci U S A* 109: 8740–8745. doi: [10.1073/pnas.1206171109](https://doi.org/10.1073/pnas.1206171109) PMID: [22592800](https://pubmed.ncbi.nlm.nih.gov/22592800/)
9. Busche MA, Eichhoff G, Adelsberger H, Abramowski D, Wiederhold KH, et al. (2008) Clusters of hyperactive neurons near amyloid plaques in a mouse model of Alzheimer's disease. *Science* 321: 1686–1689. doi: [10.1126/science.1162844](https://doi.org/10.1126/science.1162844) PMID: [18802001](https://pubmed.ncbi.nlm.nih.gov/18802001/)
10. Kuchibhotla KV, Goldman ST, Lattarulo CR, Wu HY, Hyman BT, et al. (2008) Abeta plaques lead to aberrant regulation of calcium homeostasis in vivo resulting in structural and functional disruption of neuronal networks. *Neuron* 59: 214–225. doi: [10.1016/j.neuron.2008.06.008](https://doi.org/10.1016/j.neuron.2008.06.008) PMID: [18667150](https://pubmed.ncbi.nlm.nih.gov/18667150/)
11. Minkeviciene R, Rheims S, Dobszay MB, Zilberter M, Hartikainen J, et al. (2009) Amyloid beta-induced neuronal hyperexcitability triggers progressive epilepsy. *J Neurosci* 29: 3453–3462. doi: [10.1523/JNEUROSCI.5215-08.2009](https://doi.org/10.1523/JNEUROSCI.5215-08.2009) PMID: [19295151](https://pubmed.ncbi.nlm.nih.gov/19295151/)
12. Hartley DM, Walsh DM, Ye CP, Diehl T, Vasquez S, et al. (1999) Protofibrillar intermediates of amyloid beta-protein induce acute electrophysiological changes and progressive neurotoxicity in cortical neurons. *J Neurosci* 19: 8876–8884. PMID: [10516307](https://pubmed.ncbi.nlm.nih.gov/10516307/)
13. Brown JT, Chin J, Leiser SC, Pangalos MN, Randall AD (2011) Altered intrinsic neuronal excitability and reduced Na⁺ currents in a mouse model of Alzheimer's disease. *Neurobiol Aging* 32: 2109 e2101–2114.
14. Palop JJ, Mucke L (2009) Epilepsy and cognitive impairments in Alzheimer disease. *Arch Neurol* 66: 435–440. doi: [10.1001/archneurol.2009.15](https://doi.org/10.1001/archneurol.2009.15) PMID: [19204149](https://pubmed.ncbi.nlm.nih.gov/19204149/)
15. Verret L, Mann EO, Hang GB, Barth AM, Cobos I, et al. (2012) Inhibitory interneuron deficit links altered network activity and cognitive dysfunction in Alzheimer model. *Cell* 149: 708–721. doi: [10.1016/j.cell.2012.02.046](https://doi.org/10.1016/j.cell.2012.02.046) PMID: [22541439](https://pubmed.ncbi.nlm.nih.gov/22541439/)
16. Iijima K, Liu HP, Chiang AS, Hearn SA, Konsolaki M, et al. (2004) Dissecting the pathological effects of human A β 40 and A β 42 in *Drosophila*: a potential model for Alzheimer's disease. *Proc Natl Acad Sci U S A* 101: 6623–6628. PMID: [15069204](https://pubmed.ncbi.nlm.nih.gov/15069204/)
17. Finelli A, Kelkar A, Song HJ, Yang H, Konsolaki M (2004) A model for studying Alzheimer's A β 42-induced toxicity in *Drosophila melanogaster*. *Mol Cell Neurosci* 26: 365–375. PMID: [15234342](https://pubmed.ncbi.nlm.nih.gov/15234342/)
18. Iijima K, Chiang HC, Hearn SA, Hakker I, Gatt A, et al. (2008) A β 42 mutants with different aggregation profiles induce distinct pathologies in *Drosophila*. *PLoS One* 3: e1703. doi: [10.1371/journal.pone.0001703](https://doi.org/10.1371/journal.pone.0001703) PMID: [18301778](https://pubmed.ncbi.nlm.nih.gov/18301778/)
19. Brand A, Perrimon N (1993) Targeted gene expression as a means of altering cell fates and generating dominant phenotypes. *Development* 118: 401–415. PMID: [8223268](https://pubmed.ncbi.nlm.nih.gov/8223268/)
20. Tsunoda S, Salkoff L (1995b) The major delayed rectifier in both *Drosophila* neurons and muscle is encoded by *Shab*. *Journal of Neuroscience* 15: 5209–5221. PMID: [7623146](https://pubmed.ncbi.nlm.nih.gov/7623146/)
21. Tsunoda S, Salkoff L (1995a) Genetic analysis of *Drosophila* neurons: *Shal*, *Shaw*, and *Shab* encode most embryonic potassium currents. *Journal of Neuroscience* 15: 1741–1754. PMID: [7891132](https://pubmed.ncbi.nlm.nih.gov/7891132/)
22. Lee D, O'Dowd DK (2000) cAMP-dependent plasticity at excitatory cholinergic synapses in *Drosophila* neurons: alterations in the memory mutant *dunce*. *J Neurosci* 20: 2104–2111. PMID: [10704484](https://pubmed.ncbi.nlm.nih.gov/10704484/)
23. Lee D, O'Dowd DK (1999) Fast excitatory synaptic transmission mediated by nicotinic acetylcholine receptors in *Drosophila* neurons. *J Neurosci* 19: 5311–5321. PMID: [10377342](https://pubmed.ncbi.nlm.nih.gov/10377342/)
24. Leung HT, Branton WD, Phillips HS, Jan L, Byerly L (1989) Spider toxins selectively block calcium currents in *Drosophila*. *Neuron* 3: 767–772. PMID: [2642017](https://pubmed.ncbi.nlm.nih.gov/2642017/)
25. Ping Y, Tsunoda S (2011) Inactivity-induced increase in nAChRs upregulates *Shal* K(+) channels to stabilize synaptic potentials. *Nat Neurosci* 15: 90–97. doi: [10.1038/nn.2969](https://doi.org/10.1038/nn.2969) PMID: [22081160](https://pubmed.ncbi.nlm.nih.gov/22081160/)
26. Ping Y, Waro G, Licursi A, Smith S, Vo-Ba DA, et al. (2011) *Shal*/K(v)4 channels are required for maintaining excitability during repetitive firing and normal locomotion in *Drosophila*. *PLoS One* 6: e16043. doi: [10.1371/journal.pone.0016043](https://doi.org/10.1371/journal.pone.0016043) PMID: [21264215](https://pubmed.ncbi.nlm.nih.gov/21264215/)
27. Heisenberg M, Borst A, Wagner S, Byers D (1985) *Drosophila* mushroom body mutants are deficient in olfactory learning. *J Neurogenet* 2: 1–30. PMID: [4020527](https://pubmed.ncbi.nlm.nih.gov/4020527/)
28. McGuire SE, Le PT, Davis RL (2001) The role of *Drosophila* mushroom body signaling in olfactory memory. *Science* 293: 1330–1333. PMID: [11397912](https://pubmed.ncbi.nlm.nih.gov/11397912/)
29. van Swinderen B (2009) Fly memory: a mushroom body story in parts. *Curr Biol* 19: R855–857. doi: [10.1016/j.cub.2009.07.064](https://doi.org/10.1016/j.cub.2009.07.064) PMID: [19788880](https://pubmed.ncbi.nlm.nih.gov/19788880/)
30. Tanaka NK, Tanimoto H, Ito K (2008) Neuronal assemblies of the *Drosophila* mushroom body. *J Comp Neurol* 508: 711–755. doi: [10.1002/cne.21692](https://doi.org/10.1002/cne.21692) PMID: [18395827](https://pubmed.ncbi.nlm.nih.gov/18395827/)
31. Tanaka NK, Awasaki T, Shimada T, Ito K (2004) Integration of chemosensory pathways in the *Drosophila* second-order olfactory centers. *Curr Biol* 14: 449–457. PMID: [15043809](https://pubmed.ncbi.nlm.nih.gov/15043809/)

32. Belote JM, Fortier E (2002) Targeted expression of dominant negative proteasome mutants in *Drosophila melanogaster*. *Genesis* 34: 80–82. PMID: [12324954](#)
33. Saville KJ, Belote JM (1993) Identification of an essential gene, *l(3)73Ai*, with a dominant temperature-sensitive lethal allele, encoding a *Drosophila* proteasome subunit. *Proc Natl Acad Sci U S A* 90: 8842–8846. PMID: [8415617](#)
34. Smyth KA, Belote JM (1999) The dominant temperature-sensitive lethal *DTS7* of *Drosophila melanogaster* encodes an altered 20S proteasome beta-type subunit. *Genetics* 151: 211–220. PMID: [9872961](#)
35. Madshus IH, Stang E (2009) Internalization and intracellular sorting of the EGF receptor: a model for understanding the mechanisms of receptor trafficking. *J Cell Sci* 122: 3433–3439. doi: [10.1242/jcs.050260](#) PMID: [19759283](#)
36. Longva KE, Blystad FD, Stang E, Larsen AM, Johannessen LE, et al. (2002) Ubiquitination and proteasomal activity is required for transport of the EGF receptor to inner membranes of multivesicular bodies. *J Cell Biol* 156: 843–854. PMID: [11864992](#)
37. Balut CM, Gao Y, Murray SA, Thibodeau PH, Devor DC (2010) ESCRT-dependent targeting of plasma membrane localized KCa3.1 to the lysosomes. *Am J Physiol Cell Physiol* 299: C1015–1027. doi: [10.1152/ajpcell.00120.2010](#) PMID: [20720181](#)
38. Balut CM, Loch CM, Devor DC (2011) Role of ubiquitylation and USP8-dependent deubiquitylation in the endocytosis and lysosomal targeting of plasma membrane KCa3.1. *FASEB J* 25: 3938–3948. doi: [10.1096/fj.11-187005](#) PMID: [21828287](#)
39. Hendel T, Michels B, Neuser K, Schipanski A, Kaun K, et al. (2005) The carrot, not the stick: appetitive rather than aversive gustatory stimuli support associative olfactory learning in individually assayed *Drosophila* larvae. *J Comp Physiol A Neuroethol Sens Neural Behav Physiol* 191: 265–279. PMID: [15657743](#)
40. White BH, Osterwalder TP, Yoon KS, Joiner WJ, Whim MD, et al. (2001) Targeted attenuation of electrical activity in *Drosophila* using a genetically modified K(+) channel. *Neuron* 31: 699–711. PMID: [11567611](#)
41. Benzer S (1967) Behavioral mutants of *Drosophila* isolated by countercurrent distribution. *Proceedings of the National Academy of Sciences of the United States of America* 58: 1112–1119. PMID: [16578662](#)
42. Xu Y, Condell M, Plesken H, Edelman-Novemsky I, Ma J, et al. (2006) A *Drosophila* model of Barth syndrome. *Proc Natl Acad Sci U S A* 103: 11584–11588. PMID: [16855048](#)
43. Elliott DA, Brand AH (2008) The GAL4 system: a versatile system for the expression of genes. *Methods Mol Biol* 420: 79–95. doi: [10.1007/978-1-59745-583-1_5](#) PMID: [18641942](#)
44. Bakker A, Krauss GL, Albert MS, Speck CL, Jones LR, et al. (2012) Reduction of hippocampal hyperactivity improves cognition in amnesic mild cognitive impairment. *Neuron* 74: 467–474. doi: [10.1016/j.neuron.2012.03.023](#) PMID: [22578498](#)
45. Palop JJ, Jones B, Kekoni L, Chin J, Yu GQ, et al. (2003) Neuronal depletion of calcium-dependent proteins in the dentate gyrus is tightly linked to Alzheimer's disease-related cognitive deficits. *Proc Natl Acad Sci U S A* 100: 9572–9577. PMID: [12881482](#)
46. Putcha D, Brickhouse M, O'Keefe K, Sullivan C, Rentz D, et al. (2011) Hippocampal hyperactivation associated with cortical thinning in Alzheimer's disease signature regions in non-demented elderly adults. *J Neurosci* 31: 17680–17688. doi: [10.1523/JNEUROSCI.4740-11.2011](#) PMID: [22131428](#)
47. Schaefer JE, Worrell JW, Levine RB (2010) Role of intrinsic properties in *Drosophila* motoneuron recruitment during fictive crawling. *J Neurophysiol* 104: 1257–1266. doi: [10.1152/jn.00298.2010](#) PMID: [20573969](#)
48. Choi JC, Park D, Griffith LC (2004) Electrophysiological and morphological characterization of identified motor neurons in the *Drosophila* third instar larva central nervous system. *J Neurophysiol* 91: 2353–2365. PMID: [14695352](#)
49. Kim J, Jung SC, Clemens AM, Petralia RS, Hoffman DA (2007) Regulation of dendritic excitability by activity-dependent trafficking of the A-type K⁺ channel subunit Kv4.2 in hippocampal neurons. *Neuron* 54: 933–947. PMID: [17582333](#)
50. Lugo JN, Brewster AL, Spencer CM, Anderson AE (2012) Kv4.2 knockout mice have hippocampal-dependent learning and memory deficits. *Learn Mem* 19: 182–189. doi: [10.1101/lm.023614.111](#) PMID: [22505720](#)
51. Ye CP, Selkoe DJ, Hartley DM (2003) Protofibrils of amyloid beta-protein inhibit specific K⁺ currents in neocortical cultures. *Neurobiol Dis* 13: 177–190. PMID: [12901832](#)
52. Good TA, Smith DO, Murphy RM (1996) Beta-amyloid peptide blocks the fast-inactivating K⁺ current in rat hippocampal neurons. *Biophys J* 70: 296–304. PMID: [8770205](#)

53. Jalonen TO, Charniga CJ, Wielt DB (1997) beta-Amyloid peptide-induced morphological changes coincide with increased K⁺ and Cl⁻ channel activity in rat cortical astrocytes. *Brain Res* 746: 85–97. PMID: [9037487](#)
54. Pan Y, Xu X, Tong X, Wang X (2004) Messenger RNA and protein expression analysis of voltage-gated potassium channels in the brain of Abeta(25–35)-treated rats. *J Neurosci Res* 77: 94–99. PMID: [15197742](#)
55. Pannaccione A, Secondo A, Scorziello A, Cali G, Tagliatalata M, et al. (2005) Nuclear factor-kappaB activation by reactive oxygen species mediates voltage-gated K⁺ current enhancement by neurotoxic beta-amyloid peptides in nerve growth factor-differentiated PC-12 cells and hippocampal neurones. *J Neurochem* 94: 572–586. PMID: [15969743](#)
56. Plant LD, Webster NJ, Boyle JP, Ramsden M, Freir DB, et al. (2006) Amyloid beta peptide as a physiological modulator of neuronal 'A'-type K⁺ current. *Neurobiol Aging* 27: 1673–1683. PMID: [16271805](#)
57. Kerrigan TL, Atkinson L, Peers C, Pearson HA (2008) Modulation of 'A'-type K⁺ current by rodent and human forms of amyloid beta protein. *Neuroreport* 19: 839–843. doi: [10.1097/WNR.0b013e3282ff636b](#) PMID: [18463498](#)
58. Gregori L, Fuchs C, Figueiredo-Pereira ME, Van Nostrand WE, Goldgaber D (1995) Amyloid beta-protein inhibits ubiquitin-dependent protein degradation in vitro. *J Biol Chem* 270: 19702–19708. PMID: [7649980](#)
59. Tseng BP, Green KN, Chan JL, Blurton-Jones M, LaFerla FM (2008) Abeta inhibits the proteasome and enhances amyloid and tau accumulation. *Neurobiol Aging* 29: 1607–1618. PMID: [17544172](#)
60. Hong L, Huang HC, Jiang ZF (2014) Relationship between amyloid-beta and the ubiquitin-proteasome system in Alzheimer's disease. *Neurol Res* 36: 276–282. doi: [10.1179/1743132813Y.0000000288](#) PMID: [24512022](#)
61. Schmitz A, Schneider A, Kummer MP, Herzog V (2004) Endoplasmic reticulum-localized amyloid beta-peptide is degraded in the cytosol by two distinct degradation pathways. *Traffic* 5: 89–101. PMID: [14690498](#)
62. Kumar P, Pradhan K, Karunya R, Ambasta RK, Querfurth HW (2012) Cross-functional E3 ligases Parkin and C-terminus Hsp70-interacting protein in neurodegenerative disorders. *J Neurochem* 120: 350–370. doi: [10.1111/j.1471-4159.2011.07588.x](#) PMID: [22098618](#)
63. Pannaccione A, Boscia F, Scorziello A, Adornetto A, Castaldo P, et al. (2007) Up-regulation and increased activity of KV3.4 channels and their accessory subunit MinK-related peptide 2 induced by amyloid peptide are involved in apoptotic neuronal death. *Mol Pharmacol* 72: 665–673. PMID: [17495071](#)
64. Colom LV, Diaz ME, Beers DR, Neely A, Xie WJ, et al. (1998) Role of potassium channels in amyloid-induced cell death. *J Neurochem* 70: 1925–1934. PMID: [9572276](#)
65. Yu SP, Farhangrazi ZS, Ying HS, Yeh CH, Choi DW (1998) Enhancement of outward potassium current may participate in beta-amyloid peptide-induced cortical neuronal death. *Neurobiol Dis* 5: 81–88. PMID: [9746905](#)
66. Yu SP (2003) Regulation and critical role of potassium homeostasis in apoptosis. *Prog Neurobiol* 70: 363–386. PMID: [12963093](#)
67. Diao F, Chaufy J, Waro G, Tsunoda S (2010) SIDL Interacts with the Dendritic Targeting Motif of Shal (Kv4) K⁺ Channels in Drosophila. *Molecular and Cellular Neuroscience* 45: 75–83. doi: [10.1016/j.mcn.2010.06.001](#) PMID: [20550966](#)
68. Diao F, Waro G, Tsunoda S (2009) Fast inactivation of Shal (K(v)4) K⁺ channels is regulated by the novel interactor SKIP3 in Drosophila neurons. *Mol Cell Neurosci* 42: 33–44. doi: [10.1016/j.mcn.2009.05.003](#) PMID: [19463952](#)
69. Sato H, Toyoda H, Saito M, Kobayashi M, Althof D, et al. (2013) GABA(B) receptor-mediated presynaptic inhibition reverses inter-columnar covariability of synaptic actions by intracortical axons in the rat barrel cortex. *Eur J Neurosci* 37: 190–202. doi: [10.1111/ejn.12041](#) PMID: [23134516](#)